ИНСТИТУТ ЯДЕРНОЙ ФИЗИКИ СО АН СССР

A.L. Gerasimov, F.M. Izrailev, J.L. Tennyson

SYNCHROBETATRON SIDEBAND OVERLAP IN ELECTRON-POSITRON COLLIDING BEAMS

PREPRINT 87-69

НОВОСИБИРСК

SYNCHROBETATRON SIDEBAND OVERLAP IN ELECTRON-POSITRON COLLIDING BEAMS

A.L. Gerasimov, F.M. Izrailev, J.L. Tennyson
Institute of Nuclear Physics 630090, Novosibirsk 90, USSR

TABLE OF CONTENTS

APPENDICES

SYNCHROBETATRON SIDEBAND OVERLAP IN ELECTRON-POSITRON COLLIDING BEAMS

A.L. Gerasimov, F.M. Izrailev, J.L. Tennyson
Institute of Nuclear Physics 630090, Novosibirsk 90, USSR

The detrimental influence of synchrobetatron sidebands on beam integrity is quantitatively estimated using analytic techniques. The treatment includes both the horizontal and vertical betatron oscillations and takes into account the sidebands of both parametric and coupling resonances. Two thresholds are calculated: the threshold at which betatron amplitudes begin to diffuse due to dynamical instability, and the threshold at which the rate of this diffusion becomes significant in comparison to the rate of diffusion caused by quantum fluctuations. The results may be applied to any accelerator with beam aspect ratio greater then $\sigma_x/\sigma_z = 20$.

1. Introduction

In a colliding beam storage ring, the beam-beam force is the collective, relativistically enhanced, transverse electromagnetic force experienced by a beam particle as it passes through a bunch of the opposing beam. This force gives the particle a transverse impulse, or "kick", which changes slightly the amplitudes of the vertical and horizontal betatron oscillations. Accumulated beam-beam kicks can result in an average growth of the betatron amplitudes, either via diffusion caused by a sequence of uncollelated kicks, or via resonant pumping caused by a sequence of correlated kicks. This growth can result in a loss of luminosity, beam lifetime, or both.

To estimate the cumulative effect of many beam-beam kicks, it is necessary to determine the extent to which the kicks are correlated and the nature of the correlations. This requires an analytic model and the identification of one or more transport "processes"; specific mechanisms with known statistical properties.

Beam-beam transport is a particularly complex phenomena because there appear to be several distinct processes involved. Each of these is highly sensitive to both the working parameters of the machine, and the betatron amplitudes. All of these processes involve, in one way or another, nonlinear resonances which are excited by weak couplings between the two transverse oscillations and the longitudinal motion. These couplings result from the nonlinear nature of the beam-beam force and the presence of nonlinear components in the magnet lattice of the machine. The processes themselves may be classified as either single resonance processes (such as libration effects and resonance streaming) or as multiple resonance effects (such as Arnold diffusion and synchrobetatron overlap). They have been described in a preceding review [1].

This investigation quantitatively evaluates the effects of one particular transport process: synchrobetatron sideband overlap. This process appears when the relatively low frequency synchrotron oscillations are coupled, either via the beam-beam interaction or through r.f. cavity dispersion, to the betatron oscillations. This coupling results in the splitting of each primary beam-beam resonance into a multiplet of closely spaced (in phase space) sideband resonances. Under certain conditions, e.g. when the modulation is slow enough or the beam-beam force strong enough, the sidebands can overlap, resulting in stochasticity and a "deterministic" diffusion of the betatron amplitudes.

The overlap of synchrobetatron sidebands has been examined for the one-dimensional beam-beam system in a number of preceding works [2]-[5]. The techniques used in those works have been extended, in the present study, to the full two-dimensional system. The results presented here are therefore considerably more comprehensive than those published earlier.

An investigation of dynamical instability requires a specific model. The model used in this analysis makes use of the so-called "weak-strong" beam approximation. This approximation assumes that the current distribution in the "opposing" beam is a constant, and that the beam-beam force is an independent function of the two transverse coordinates x, z, and time. The weak-strong beam assumption precludes the presence of "coherent effects" which require a self-consistent or strong-strong beam model. These effects, in most existing machines, are considered to be negligible in comparison to the effects investigated below. The quantitative calculations are performed by computer. Because some of these calculations are lengthy, it is convenient to represent the beam-beam force with a simple analytic approximation to the exact force that would exist were the beam density profile precisely bi-Gaussian. This approximation to the Gaussian force has been shown to be accurate enough to produce reliable estimates of resonance characteristics in all regions of the amplitude plane [6]. Since the beam is not expected to be precisely Gaussian anyway, a force representing an almost Gaussian distribution is considered to be as good an estimate as the Gaussian itself. A description of the model is given in Appendix B.

Synchrobetatron sidebands arise when there is coupling between the longitudinal synchrotron oscillations and the transverse betatron oscillations. This coupling causes the primary beam-beam resonances to break into a multiplet of sideband resonances. There are three common coupling mechanisms: non-zero chromaticity (resulting in tune modulation), non-zero dispersion at the intersection points (resulting in modulation of the betatron oscillation center), and finite bunch length (resulting in tune-shift modulation). All of these mechanisms result in a swaying of the primary betatron resonances back and forth in the amplitude plane. The magnitude and frequency of this swaying, together with the width and frequency of the primary resonance, completely determine the characteristics of the sidebands. Thus, the precise cause of the swaying is largely irrelevant in determining its effect on particle transport. In the analysis that follows, the mechanism used to illustrate synchrobetatron coupling is tune modulation (non-zero chromaticity). This is known to be the primary coupling mechanism at VEPP-4, and is the simplest mechanism to treat analytically. The results are easily extended to the case of tune-shift modulation, as described in section 5.

This paper is limited to an investigation of the nature of dynamical instability in the model system, as it depends on the various parameters in the system. It is not concerned directly with the problems of beam blow-up and reduction of lifetime, both of which might result from the presence of instability.

The study is broken roughly into three parts: the first investigates the threshold conditions for instability in the model system, the second looks at the diffusion rate that characterizes the instability, and the third analyses the extent to which instability can be avoided by selecting an optimal working tune.

2. The Model System

The model system is defined by the Hamiltonian

$$H(I_x,I_z,\theta_x,\theta_z) = I_x\{\bar{\omega}_{ox}+M_x\sin(\Omega t)\} + I_z\{\bar{\omega}_{oz}+M_z\sin(\Omega t)\} + \delta_t V(x,z) \quad (1)$$

where
$$\delta_t \equiv \sum_{n=-\infty}^{\infty} \delta(t-n) \quad (2)$$

The amplitudes of the horizontal and vertical tune modulations are M_x and M_z, while the frequency of modulation is Ω (the synchrotron frequency). The average betatron frequencies are $\bar{\omega}_{ox}$ and $\bar{\omega}_{oz}$. The term $\delta_t\ V(x,z)$ represents the beam-beam impulse that is given to the particle every time it passes an interaction point. At an interaction point, the coordinates x and z are related to $(I_x,I_z,\theta_x,\theta_z)$ via the relations

$$\begin{aligned} x &= (2I_x\beta_x)^{1/2}\ \cos\theta_x \\ z &= (2I_z\beta_z)^{1/2}\ \cos\theta_z \end{aligned} \quad (3)$$

where β_x and β_z are the machine beta-functions at the interaction points. The actions I_x, I_z are thus related to the betatron amplitudes A_x, A_z by

$$\begin{aligned} A_x &= (2I_x\beta_x)^{1/2} \\ A_z &= (2I_z\beta_z)^{1/2} \end{aligned} \quad (4)$$

It is convenient to introduce the normalized amplitudes a_x and a_z defined by

$$\begin{aligned} a_x &\equiv A_x/\sigma_x \\ a_z &\equiv A_z/\sigma_z \end{aligned} \quad (5)$$

where σ_x and σ_z are the RMS beam width and height. The horizontal and vertical tune shifts ξ_x and ξ_z are proportional to the auxiliary constants β_x and β_z. If the beam current is fixed at a certain value, the tune shifts are related to the beta functions by (see appendix A)

$$\begin{aligned} \xi_x &= \beta_x/\sigma_x \\ \xi_z &= \beta_z/\sigma_z \end{aligned} \quad (6)$$

The beam-beam potential V(x,z) is represented in this work by the approximate

analytic model described in appendix B. It is independent of the tuneshifts, with a parametric dependence on the beam aspect ratio σ_x/σ_z only.

The characteristics of nonlinear resonances were first described for general multi-dimensional oscillator systems by Chirikov [7]. The characteristics of the primary beam-beam resonances and their sideband multiplets are reviewed in appendices D and E. The characteristics depend on the above mentioned parameters and the beam-beam potential $V(x,z)$. They can be expressed conveniently in terms of two intermediate functions, the Fourier tranform $F_{\underline{m}}(I_x,I_z)$ of $V(x,z)$ (transformed with respect to θ_x and θ_z), and the nonlinearity $\Lambda_{\underline{m}}(I_x,I_z)$. These are defined by

$$F_{\underline{m}}(\underline{I}) \equiv \frac{1}{(2\pi)^2}\int_0^{2\pi} d\theta_x \int_0^{2\pi} d\theta_z \cos(m_x\theta_x + m_z\theta_z)\ V(I_x,I_z,\theta_x,\theta_z) \qquad (7)$$

$$\Lambda_{\underline{m}}(\underline{I}) \equiv 2\, m_x m_z \frac{\partial^2 F_o}{\partial I_x \partial I_z} + m_x^2 \frac{\partial^2 F_o}{\partial I_x^2} + m_z^2 \frac{\partial^2 F_o}{\partial I_z^2} \qquad (8)$$

where $F_o \equiv F_{\underline{m}=0,0}$ and $\underline{I}$ and $\underline{m}$ denote the pairs (I_x,I_z) and (m_x,m_z). The amplitude-dependent frequencies ω_x and ω_z are defined to be

$$\omega_x(\underline{I}) \equiv \bar{\omega}_{xo} + \frac{\partial F_o(\underline{I})}{\partial I_x} \qquad (9)$$

$$\omega_z(\underline{I}) \equiv \bar{\omega}_{zo} + \frac{\partial F_o(\underline{I})}{\partial I_z} \qquad (10)$$

The sidebands are characterized by two additional parameters, the modulation frequency Ω and the multiplet width in frequency

$$\omega_M \equiv m_x M_x + m_z M_z$$

Most of the resonance characteristics refer to displacements in action space. In the following list, they are expressed in terms of changes in the "resonant action" J_1 defined in Appendix C. Given some displacement ΔJ_1, the corresponding displacements in I_x and I_z are

$$\Delta I_x = m_x\, \Delta J_1$$
$$\Delta I_z = m_z\, \Delta J_1 \qquad (11)$$

3. Resonance Characteristics

The following expressions for the characteristics of the primary and sideband resonances are derived in appendices D and E, respectively.

1. Location of the $\underline{m}$th resonance in action (I_x,I_z) space. The location is given by the condition

$$m_x\omega_x(\underline{I}) + m_z\omega_z(\underline{I}) + 2\pi n = 0 \qquad (12)$$

2. Resonance width ΔJ_1

$$\Delta J_1 = 4\sqrt{|2\, F_{\underline{m}}/\Lambda_{\underline{m}}|} \qquad (13)$$

3. Frequency of small amplitude resonant libration $\omega_{\underline{m}}$

$$\omega_{\underline{m}} = \sqrt{|2\, F_{\underline{m}}\, \Lambda_{\underline{m}}|} \qquad (14)$$

4. Sideband spacing $\Delta^S J_1$.

$$\Delta^S J_1 = \Omega\ /\ \Lambda_{\underline{m}} \qquad (15)$$

5. Average sideband width $\langle \Delta^W J_1 \rangle$.

$$\langle \Delta^W J_1 \rangle = \Delta J_1 \left| \frac{\Omega}{\pi\omega_M} \right|^{1/4} \qquad (16)$$

6. Multiplet width $\Delta^M J_1$.

$$\Delta^M J_1 = 2\,\omega_M\ /\ \Lambda_{\underline{m}} \qquad (17)$$

These six resonance characteristics are illustrated in Figs. 1-3. They provide the basis for the following study of the instability thresholds and diffusion rates.

4. Thresholds and Diffusion Rates

There are three regimes which characterize diffusion across the sideband multiplet (diffusion along the multiplet is usually small enough that it can be neglected in the presence of quantum fluctuations). The first regime corresponds to the non-overlapping condition, the second (intermediate) regime to quasilinear diffusion, and the third to adiabatic diffusion. The thresholds separating the three

regimes are derived in appendix F. The quasilinear diffusion rate is calculated in appendix G.

4a. Diffusion Regime Thresholds

The threshold for sideband overlap, equation (F4), is given by the condition

$$|2F_{\underline{m}}\Lambda_{\underline{m}}|^2 > \left|\frac{\omega_M \Omega^3}{2(2\pi)^3}\right| \qquad (18)$$

The threshold for adiabatic diffusion is given by (F13)

$$|2F_{\underline{m}}| > \left|\frac{\omega_M \Omega}{\Lambda_{\underline{m}}}\right|$$

or

$$|2F_{\underline{m}}\Lambda_{\underline{m}}| > |\omega_M \Omega| \qquad (19)$$

There is, of course, a region where (19) is satisfied and (18) is not. But in this region

$$(\omega_M\Omega)^2 < \left|\frac{\omega_M \Omega^3}{2(2\pi)^3}\right|$$

or

$$|2\omega_M/\Omega| < 1/(2\pi)^3 \approx .004 \qquad (20)$$

This means, from (E29), that the number of sidebands in the multiplet is .004. Since for sidebands to overlap there must be at least two in the multiplet, this region is completely stable and the diffusion rate is zero.

4b. Quasilinear Diffusion Rate

The quasilinear diffusion rate (the diffusion rate in the region of parameter space where (18) is satisfied but (19) is not) for the random variable J_1 is given by equation (G3)

$$D_{ql} = \left|\frac{(2F_{\underline{m}})^2}{\omega_M}\right| \qquad (21)$$

The diffusion rates for the amplitude variables a_x and a_z are given by (G4)

$$D(a_x) = \left[m_x \frac{\partial a_x}{\partial I_x}\right]^2 D_{ql} = \left[\frac{m_x \xi_x}{a_x \sigma_x}\right]^2 D_{ql}$$

$$D(a_z) = \left[m_z \frac{\partial a_z}{\partial I_z}\right]^2 D_{ql} = \left[\frac{m_z \xi_z}{a_z \sigma_z}\right]^2 D_{ql} \qquad (22)$$

In electron-positron machines, the adiabatic diffusion regime is seldom entered. For this reason, and because the adiabatic rate is always less than the quasilinear rate, the adiabatic regime may be safely ignored in electron-positron machines (this may not be true for proton-antiproton colliders).

The dynamical diffusion rate (22) is only significant if it is stronger than the pre-existing diffusion caused by quantum fluctuations. The condition, for i= x or z, is

$$D(a_i) > D_{qf} = 1/T_d$$

where D_{qf} is the diffusion rate due to quantum fluctuations and T_d is the damping time. More explicitly, from (21) and (22), this condition is

$$\left[\frac{m_i \xi_i}{a_i \sigma_i}\right]^2 \left|\frac{(2F_{\underline{m}})^2}{\omega_M}\right| > 1/T_d \qquad (23)$$

To estimate the effect of instability on the beam integrity of a particular machine; it is necessary to both determine the conditions under which the sidebands of a particular resonance $\underline{m}$ overlap and the rate of quasilinear diffusion induced by this overlap. If overlap does in fact occur for typical parameter values of the machine, and if the diffusion rate is comparable to or greater than the diffusion induced by quantum fluctuations, then the resonance in question must adversally affect at least the beam size, and possibly the beam lifetime.

5. Quantitative Analysis

To simplify the results of the analysis (though not the analysis itself), and because it corresponds roughly to the actual situation in VEPP-4, we consider only the case in which M_x=0. The modulation amplitude is then given by M_z. For reference parameter values we use the operating conditions of VEPP-4: ξ_z/ξ_x=4, σ_x/σ_z=80, P=2π/Ω=50, M_z=.015 and a damping time of T_d=1000 revolutions.

To maximize the intuitive utility of the numerical results, the parametric dependences of the threshold conditions (18) and (23) are split. In both cases, the dependences on the amplitude $\underline{a}$, the resonance $\underline{m}$, the ratio ξ_x/ξ_z and the ratio σ_x/σ_z are moved to the left hand side, while the dependencies on M_z, Ω, ξ_z and

T_d are moved to the right hand side. The condition (18) for overlap then becomes

$$OP1 > OP2 \tag{24}$$

where
$$OP1(\underline{a},\underline{m},\xi_x/\xi_z,\sigma_x/\sigma_z) \equiv 2\,(2F_{\underline{m}}\Lambda_{\underline{m}})^2/\,(\xi_z{}^4\,m_z) \tag{25}$$

$$OP2(\Omega,M,\xi_z) \equiv M_z\,/\,(P^3\xi_z{}^4) \tag{26}$$

and $P \equiv 2\pi/\Omega$ is the modulation period. The condition for significant dynamical diffusion in the vertical direction (23) becomes

$$DP1 > DP2 \tag{27}$$

where
$$DP1(\underline{a},\underline{m},\xi_x/\xi_z,\sigma_x/\sigma_z) \equiv \frac{(2F_{\underline{m}})^2\,m_z}{(a_z\sigma_z)^2} \tag{28}$$

and
$$DP2(T_d,M_z,\xi_z) \equiv \frac{M_z}{T_d\,\xi_z{}^2} \tag{29}$$

The parameters OP1 and DP1 appear to depend only weakly on the tune-shift ratio ξ_x/ξ_z and the aspect ratio σ_x/σ_z for most resonances. Thus OP1 and DP1 are fairly machine independent and can be applied to a wide range of electron-positron machines with elliptical beams.

In the tops of Figs. 4-6, the functions OP1 (curved lines) and OP2 (straight lines, except in Fig. 6) are plotted against vertical amplitude at five different values of the horizontal amplitude: a_x=0,1,2,3,4. Sideband overlap occurs where OP1 > OP2. In the bottoms of Fig.s 4-6, the functions DP1 and DP2 are plotted against vertical amplitude for the same horizontal amplitudes as the top plots. Again dynamical diffusion excedes quantum diffusion when DP1 > DP2. On each plot, three cases of OP2 and DP2 are shown for comparison. In each case, M_z, Ω, and T_d are the same, while ξ_z takes on three different values ξ_z= .03, ξ_z= .06, and ξ_z= 10.

By looking at the graphs, it is possible to see which resonances overlap at which amplitudes, and at which vertical tune shifts ξ_z. To make the same comparison for other machines with different modulations and damping times, its only necessary to adjust the lines OP2 and DP2 according to the formulas (26) and (29).

Figure 4 shows the case where a_x=0. Since all coupling resonances have zero width here, only the vertical parametric resonances with m_z=2 to 20 are shown. The parameter DP2 is proportional to the diffusion induced by the quantum fluctuations. This diffusion rate is sufficient to counter the radiation damping at amplitudes smaller than a_z=1, but because the damping is proportional to

amplitude, it is not sufficient to counter damping at larger amplitudes. Therefore, even if the dynamical diffusion rate were twice the quantum fluctuation rate, it could not easily transport particles beyond a_z=2 (much less to a_z=10 or a_z= 20). So for reference purposes, a straight slanted line is drawn into the lower plot of Fig. 4. This line corresponds to the function $DP2 \times a_z{}^2$ and gives the threshold at which the dynamical diffusion rate (represented by DP1) would be strong enough to push a particle to a_z when ξ_z=.06.

Figures 5a-d include coupling resonances as well as parametric, but are restricted to 6th, 8th, and 10th order resonances only (the order of a resonance is the integer $OR = |m_x| + |m_z|$). At each value of a_x, these resonances are separated for clarity of illustration into four groups. Each group is associated with a value of m_x, with m_x =0,2,4, or 6.

While Figs. 4 and 5 represent the case of tune modulation, the case of tune-shift modulation is shown in Fig. 6. Tune-shift modulation differs from tune modulation only in that the amplitude of tune modulation is dependent on the betatron amplitude a_z; specifically, M_z becomes proportional to the amplitude-dependent tune-shift, which from (9) is given by

$$\Delta\omega_z(\underline{I}) = \frac{\partial F_0(\underline{I})}{\partial I_z}$$

This only affects OP2 and DP2. Since both of these functions are proportional to M_z, they are also proportional to $\Delta\omega_z(\underline{I})$. This, and the fact that tune-shift modulation is identical to tune modulation at small amplitudes, allows for straightforward modifications to OP2 and DP2

$$OP2(\Omega,M,\xi_z,a_z) \equiv \frac{M_{zo}}{P^3\xi_z{}^4}\,\frac{\Delta\omega_z(a_z)}{\xi_z} \tag{30}$$

$$DP2(T_d,M_z,\xi_z,a_z) \equiv \frac{M_{zo}}{T_d\,\xi_z{}^2}\,\frac{\Delta\omega_z(a_z)}{\xi_z} \tag{31}$$

where M_{zo} is the amplitude of the tune-shift modulation $M_{zo}=\Delta\xi_z/2$.

Note that since both OP2 and DP2 are proportional to M_z, small modulation amplitudes have lower overlap thresholds and faster diffusion rates than large modulation amplitudes. The apparent paradox at very small modulation amplitudes is resolved by the fact that the validity of the threshold conditions (18) and (23) depends on there being more than one sideband in the multiplet. Since from (E29) the number of sidebands is $2m_zM_z/\Omega$, the above analysis breaks down when

$$M_z < \Omega/(2m_z) \tag{32}$$

When this happens, resonance overlap, and thus dynamical diffusion, becomes

impossible exccpt at very high tune shifts. Equation (30) is therefore a criterion for the elimination of synchrobetatron instability. Parametric resonances of order greater than about m_z=16 are harmless, so a safe criterion is $M_z < \Omega/32$.

6. Discussion of Results

For the purposes of this discussion, it is useful to refer to resonances in terms of their order $OR = |m_x| + |m_z|$ and slope in the frequency plane $SL = m_x/m_z$.

Two resonances with the same slope but different order are similar in many respects. Their resonance conditions (12) and locations in the amplitude plane are identical. As a rough rule of thumb, the Fourier transform $F_{\underline{m}}$ falls off exponentially with increasing order, the transforms of resonances at each order being about 10 times smaller than those of resonances at the preceding order. From (13) and (16) it follows that the sideband width is reduced by about a factor of three each time the order is increased by one. This rule is generally valid at intermediate amplitudes; the differences are greater than this at small amplitudes and smaller than this at large amplitudes.

Two resonances of the same order but different slopes may have very different characteristics, and these differences depend strongly on the amplitude. For example, when $a_x << 1$, only resonances with $SL << 1$ are significant while when $a_z << 1$, only resonances with $SL >> 1$ are significant. When $a_x \approx a_z$, at least at intermediate amplitudes, the resonances of all slopes are of about equal strengths. Again, this rule breaks down at large amplitudes where resonances with $SL \approx 1$ dominate and at small amplitudes where resonances with $SL << 1$ and $SL >> 1$ dominate.

The overlap parameter OP1, for all of the resonances shown, peaks at an intermediate vertical amplitude $2 < a_z < 8$ with high order resonances peaking at higher amplitudes than low order resonances. The highest values of OP1 are obtained for the parametric resonances $SL = 0$ at small horizontal amplitudes. This suggests that dynamical diffusion in a machine with a highly linear lattice appears first at about $a_z = 5$ and $a_x = 0$ (this result could be altered by the presence of strong machine nonlinearities, which were not taken into account in this study).

A typical high order resonance is the (0,10), shown in figure 4. The sidebands of this resonance begin to overlap at $a_z \approx 5$ when the vertical tune shift reaches $\xi_z \approx .03$. The diffusion due to this overlap (from the bottom plot) becomes significant at $\xi_z \approx .04$, but only at larger amplitudes $8 < a_z < 15$. By the time ξ_z reaches .06, the 10th order sidebands overlap in the interval $2 < a_z < 25$ with strong diffusion in the interval $5 < a_z < 25$. Although 10th order resonances can be avoided, 20th order parametric resonances cannot be when $\xi_z \geq .05$. These begin to overlap at $a_z \approx 10$ when $\xi_z = .06$.

Generally speaking, because the synchrobetatron instability affects only intermediate amplitudes, its effect on either luminosity or lifetime is questionable. In the case of luminosity, only the easily avoidable 8th order resonances can overlap at amplitudes below $a_z = 2$, and even these have an insufficient diffusion rate at $a_z = 2$ to have any real effect. Since for beam blowup to occur, the diffusion rate must increase substantially at $a_z = 2$, its unlikely that this mechanism is responsible for beam blow-up. Furthermore, since at large amplitudes (see Fig. 4) the dynamical diffusion rate appears to be insufficient to counter radiation damping, its also unlikely that this mechanism can account for particle loss on apertures at $a_z > 30$ (apertures below $a_z = 20$ could probably be reached). One experimental observation that does appear to be explainable by this mechanism is the appearance of long "tails" on the transverse density distributions [8].

It should be noted that the modulation amplitude M_z depends on the synchrotron amplitude, and that this tends to diffuse at some characteristic rate. If the value M_z used here is interpreted to be the maximum modulation amplitude, then any lower value is also accessible to the particle and will be realized within about a damping time. As mentioned above, the diffusion rate increases as M_z drops until resonance overlap fails altogether due to a deficiency of sidebands in the multiplet. It is therefore necessary to know approximately how many sidebands there are in the multiplets. Since this number is $2m_z M_z/\Omega$, using the above values with $m_z = 10$ gives 2.4 sidebands. It follows that when $m_z < 4$, the deficiency of sidebands in the multiplet inhibits the appearance of instability at the thresholds indicated by the condition (18).

The results illustrated in the top plots of Figs. 4-5 are summarized in Figs. 7a-f. In each of these figures, the dangerous resonances at a particular horizontal amplitude a_x are depicted in two ways. Firstly, the lines of dangerous resonances are drawn into the tune plane to show their density. Resonances that produce instability at tune shifts below $\xi_z = .03$ are represented by lines with double thickness. Secondly, the locations of the dangerous resonances are shown in the discrete resonance vector space $\underline{m}$. In the latter space, resonances are differentiated by four different symbols, indicating the tune shift at which they produce instability. Figures 7a-e show the dangerous resonances associated with the five amplitudes $a_x = 0,1,2,3,4$ separately, while Fig. 7f shows the combined group of all dangerous resonances. Figures 7a-e show clearly the increase in the influence of the coupling resonances as a_x is increased, and the simultaneous decrease in the influence of the parametric resonances. It is apparent from Fig. 7f that the vertical parametric resonances are in general far more dangerous than the coupling resonances (this is due, to a certain extent, to our restriction $M_x = 0$). Finally, even when only the the most dangerous resonances are considered (those that produce overlapping sidebands below $\xi_z = .03$), it is not easy to find a hole in the tune plane of Fig. 7f big enough for a beam with a tune spread greater than $\xi_z = .05$.

7. Conclusions

This study gives an indication of the extent to which dynamical diffusion plays a significant role in the beam-beam limit. It is comprehensive in that it considers the dependence of sideband overlap and dynamical diffusion rates on the vertical and horizontal betatron amplitudes, the synchrotron amplitude, the modulation amplitude, the modulation frequency, the tune-shifts, and the full range of parametric and coupling resonances excited by the beam-beam interaction.

It cannot, by itself, be used to predict luminosity and lifetime since it does not take into account other known transport mechanisms. Furthermore, this study includes only beam-beam contributions to the nonlinearity $\Lambda_{\underline{m}}$ and the resonance strength $F_{\underline{m}}$. In most electron- positron colliders, there are significant nonlinear elements in the magnet lattice which also contribute to $\Lambda_{\underline{m}}$ and $F_{\underline{m}}$. The lattice contributions are typically negligible at small amplitudes ($a_{x,z}<5$) but can easily dominate at large amplitudes ($a_z > 20$).

Taking into account the above mentioned limitations, this analysis is fairly conclusive on several points. Firstly, its clear that the parametric resonances ($m_x=0$) are the first to produce dynamical diffusion and are therefore the most dangerous resonances at each order. At tenth order, for example, only the (0,10) resonance is dangerous; other coupling resonances of the same order are not capable of inducing diffusion at realistic tune-shifts. Secondly, in the absence of lattice resonances and nonlinearities, dynamical diffusion appears first at intermediate amplitudes above two sigma and below ten sigma. Thirdly, the sign of a resonance's slope in frequency space is not important (only its absolute magnitude is significant). So for sideband overlap, there is little difference between sum and difference resonances in highly elliptical beams. Fourthly, dynamical diffusion rates for all but easily avoidable low order resonances appear to be insufficient to cause either beam blow up (at small amplitudes) or particle loss (at large amplitudes). Dynamical diffusion could be responsible for extended "tails" on the transverse density profile of the beam.

Taken together, these results imply that the dynamical diffusion induced by the beam-beam interaction is, by itself, incapable of affecting beam luminosity or beam lifetime to the extent observed in VEPP-4. It is therefore believed that either single resonance (non-chaotic) effects play a more important role in the beam-beam limit, or that the resonance strengths calculated in this analysis have been substantially underestimated due to the omission of nonlinear multipole moments in the magnet lattice and other nonlinear forces.

This work was principally supported by the National Academy of Sciences and the Soviet Academy of Science under the terms of the US-USSR Interacademy Agreement on Scientific Exchange and Cooperation. The authors would also like to thank Queen Mary College and CERN for significant additional support.

Fig. 1: Resonance location and width in action space. The resonance is centered on the line defined by the resonance condition (12), the direction of resonant oscillation is given by the vector $\underline{m}$ (D6), and the width of the resonance is given by (11) and (13).

Fig. 2: Phase space portrait of a nonlinear resonance. The resonance width (13) is the full separatrix width. The frequency of small amplitude oscillation is the frequency of phase oscillation when the particle is close to the center of the resonance (analogous to the small amplitude frequency of a pendulum). Since the invariant tori are three dimensional surfaces in the five dimensional phase space, this portrait is a section of co-dimension two, corresponding to fixed values of the revolution phase (equated in this work with time) and some betatron phase other than Ψ_1.

Fig. 3: Phase space portrait of a sideband multiplet. Synchrotron modulation of the betatron motion has increased the temporal periodicity of the Hamiltonian, resulting in the formation of sideband multiplets where formerly there were single resonances. The sideband spacing (15) is proportional to the synchrotron frequency Ω, while the multiplet width (17) is proportional to the modulation amplitude M. The section is similar to that in Fig. 2, except that it is taken at a fixed value of the modulation phase instead of the revolution phase. Note that although strict temporal periodicity does not exist if the ratio of modulation frequency to revolution frequency is not rational (making it difficult to plot these portraits, even with a computer), an irrational ratio does not preclude the existence of these invariant tori.

Fig. 4: Sideband overlap thresholds and thresholds of significant diffusion for the vertical one dimensional resonances at zero horizontal amplitude. The top figure shows plots of OP1 (25) (curved lines) and OP2 (26) (straight lines) as a function of amplitude for different resonances and tune shifts respectively. Sideband overlap occurs where OP1>OP2. The bottom figure shows plots of DP1 (28) (curved lines) and DP2 (29) straight lines. The dynamical diffusion rate excedes the quantum fluctuation rate when DP1>DP2. In this figure, as well as in Fig.s 5 and 6, the tune shift ratio is TSz/TSx =4, the aspect ratio is $ASR=\sigma_x/\sigma_z=80$, the period of synchrotron modulation is PD=50, the modulation amplitude is $AM=\Delta\upsilon_z=\Delta\omega_z/2\pi=.015$, and the damping time is DT=1000 revolutions.

Fig.5: Sideband overlap thresholds and thresholds of significant diffusion for coupling resonances at fixed non-zero horizontal amplitudes. As in figure 4, the top figure shows plots of OP1 and OP2 while the bottom figure shows DP1 and DP2. Sideband overlap occurs where OP1>OP2 and dynamical diffusion excedes quantum diffusion when DP1>DP2. Sixth, eighth, and tenth order resonances are shown, but are separated, for clarity of illustration, into groups distinguished by the values of m_x. Each value of horizontal amplitude is represented by four groups, or pairs of figures. Four different horizontal amplitudes are represented altogether: Ax = 1,2,3,4.

Fig. 6: Overlap and diffusion rate thesholds for the case of tune shift modulation. Figs. 4 and 5 represent the case of tune modulation. If the tune shift is modulated instead, th· modulation amplitude M becomes dependent on amplitude, going to zero as the ampitude goes to infinity. This results in modifications of the graphs of OP2 and DP2, causing them to bend downward at large amplitudes. Thus tune shift modulation can be more dangerous, at least at large amplitudes, than tune modulation.

Fig. 7: Dangerous resonances as a function of horizontal amplitude. Using the graphs from Figs. 4 and 5, the resonances capable of inducing diffusion via sideband overlap are illustrated both in the tune plane and in the discrete resonance vector space m. In the latter space, resonances that overlap are differentiated by four different symbols. The dots indicate resonances that do not overlap, even at ξ_z=.1. The circles indicate resonances that overlap when .1>ξ_z>.06, dots within squares indicate resonances that overlap when .06>ξ_z>.03, and circles within squares indicate resonances that overlap when .03>ξ_z. Figures 7a-e show the five cases A_x=0,1,2,3,4 separately, with Fig. 7f showing the dangerous resonances at all amplitudes.

APPENDIX A: Parameter Relationships; the Jacobian

The Hamiltonian of the beam-beam system has the form

$$H = I_x\omega_{ox} + I_z\omega_{oz} + \Sigma\,\delta(t-n)\,V(x,z) \qquad (A1)$$

The horizontal position x and momentum p_x are related to the horizontal action I_x and angle θ_x by

$$\begin{aligned} x &= (2I_x\beta_x)^{1/2}\cos\theta_x \\ p_x &= (2I_x/\beta_x)^{1/2}\sin\theta_x \end{aligned} \qquad (A2)$$

so the betatron amplitude A_x is related to the action by

$$A_x = (2I_x\beta_x)^{1/2} \qquad (A3)$$

The change in amplitude δA_x and change in phase $\delta\theta_x$ associated with a change in momentum δp_x (x held constant) is given by

$$\begin{aligned} \delta A_x &= \delta p_x\,\beta_x\sin\theta_x \\ \delta\theta_x &= \delta p_x\,\beta_x\cos\theta_x / A_x \end{aligned} \qquad (A4)$$

Since both δp_x and δp_z are proportional to V(x,z), and therefore to the beam current i, it follows that the tune shifts ξ_x and ξ_z can be changed by altering either the current i or the beta functions β_x and β_z. In fact, all of the resonance characteristics depend only on the two parameters $i\beta_x$ and $i\beta_z$. It is therefore possible, and in the interest of algebraic economy, to keep the current (and therefore the potential V(x,z)) fixed, and adjust the tuneshifts with the beta functions alone. Accordingly, it will be assumed that V(x,z) is fixed such that, for any tune shifts ξ_x and ξ_z, when x,z << 1,

$$\lim_{\substack{x\to0\\z\to0}}\frac{\partial V(x,z)}{\partial x} = \frac{4\pi x}{\sigma_x}\;;\qquad \lim_{\substack{z\to0\\x\to0}}\frac{\partial V(o,z)}{\partial z} = \frac{4\pi z}{\sigma_z} \qquad (A5)$$

The Jacobian relating the action to the amplitude is

$$\frac{dI_x}{dA_x} = \frac{A_x}{\beta_x} \qquad (A6)$$

From Hamilton's equations, the instantaneous jump in momentum due to the beam-beam kick is...

$$\Delta p_x = \frac{-\partial V}{\partial x}$$

at small x,z this is

$$\Delta p_x = -4\pi x/\sigma_x$$
$$\Delta p_z = -4\pi z/\sigma_z \qquad (A7)$$

If the beta functions are one, i.e. the orbit is a circle in the phase plane, then the tune shifts are just $\xi_x = 1/\sigma_x$, $\xi_z = 1/\sigma_z$. The tune shifts are determined by the beta functions according to

$$\xi_x = \beta_x/\sigma_x \; ; \quad \xi_z = \beta_z/\sigma_z \qquad (A8)$$

Note that the units of measurement in the x and z planes are identical above. If, instead, x and z are normalized to σ_x and σ_z, then using the normalized amplitudes

$$a_x = A_x/\sigma_x$$
$$a_z = A_z/\sigma_z$$

the Jacobian diagonal elements for the normalized coordinates are

$$\frac{dI_i}{da_i} = \frac{a_i\,\sigma_i^2}{\beta_i} = \frac{a_i\sigma_i}{\xi_i} \qquad (A9)$$

APPENDIX B: Beam-Beam Model

The approximate analytic model is defined by the potential

$$V(x,z) = \frac{A}{f(z) + g(x)} - F \ln [\, h(z,x) \,] \qquad (B1)$$

where

$$f(z) = \sqrt{z^2 + B} + Cz^2$$
$$g(x) = D \exp(+x^2/E)$$
$$h(z,x) = (x^2 + z^2 + G)$$

and

A=11.48 B=2. (σ_z/σ_x) C=.6
D=.82 E=4. F=6.6
G=2.3

The beam-beam kicks are given by

$$\Delta p_x = \xi_x \frac{\partial V}{\partial x}$$
$$\Delta p_z = \xi_z \frac{\partial V}{\partial z} \qquad (B2)$$

APPENDIX C: Resonance Coordinates

The resonance Hamiltonian includes only one Fourier term of the full transformed Hamiltonian (D3) and (I4)

$$H_{\underline{m},n} = H_0(\underline{I}) + 2\,F_{\underline{m}}(\underline{I}) \cos(m_x\theta_x + m_z\theta_z + 2\pi n t) \qquad (C1)$$

This Hamiltonian describes an integrable system and can therefore be transformed into a new Hamiltonian with only one degree of freedom. A canonical transformation replaces the old action-angle variables $\underline{I}$, $\underline{\theta}$ by new variables $\underline{J} = \{J_1, J_2\}$, and $\underline{\Psi} = \{\Psi_1, \Psi_2\}$. The linear generating function for this transformation is given by

$$G = \underline{I}_0 \cdot \underline{\theta} - \underline{J} \cdot \mu \cdot \underline{\theta} + J_1 2\pi n t \qquad (C2)$$

where $\underline{I}_0 = (I_{0x}, I_{0z})$ is an arbitrary point in action space and μ is a 2x2 tensor of the form

$$\mu \equiv \begin{vmatrix} \mu_{xx} & \mu_{zx} \\ \mu_{xz} & \mu_{zz} \end{vmatrix}$$

The new coordinates are then defined by the relations

$$\Psi_1 \equiv \frac{\partial G}{\partial J_1} \qquad \Psi_2 \equiv \frac{\partial G}{\partial J_2}$$
$$I_x = \frac{\partial G}{\partial \theta_x} \qquad I_z = \frac{\partial G}{\partial \theta_z} \qquad (C3)$$

and the new Hamiltonian by

$$K(\underline{J}, \underline{\Psi}) = H(\underline{I}, \underline{\theta}) + \partial G/\partial t \qquad (C4)$$

Since we want J_2 to be an invariant of (C1), we choose the components of μ to be such that Ψ_2 will be absent from the transformed Hamiltonian, i.e. such that (C3) gives

$$\Psi_1 = m_x\theta_x + m_z\theta_z + 2\pi n t \qquad (C5)$$

The appropriate choice is $\mu_{xx} = m_x$ and $\mu_{zx} = m_z$ (see appendix J). This specification alone (leaving μ_{xz} and μ_{zz} unspecified) results in the following additional identities:

$$J_2 = [m_x(I_{oz} - I_z) - m_z(I_{ox} - I_x)] \,/\, \mathrm{Det}\ \mu \qquad (C6)$$

and, when $J_2=0$,

$$\begin{aligned} \Delta I_x &\equiv (I_x - I_{ox}) = m_x J_1 \\ \Delta I_z &\equiv (I_z - I_{oz}) = m_z J_1 \end{aligned} \qquad (C7)$$

The new transformed Hamiltonian is found by setting the invariant J_2 to zero (using (C6) to find either the appropriate point $\underline{I}_o$ or alternatively the appropriate initial conditions), replacing I_x and I_z in (C1) by $m_xJ_1+I_{ox}$ and $m_zJ_1+I_{oz}$, replacing the phase in (C1) by Ψ_1 as shown in (C5), and adding $J_1 2\pi n$ as specified in (C4).

$$K(J_1,\Psi_1) = H_o(J_1) + 2\,F_{\underline{m}}(J_1)\cos\Psi_1 + J_1 2\pi n \qquad (C8)$$

It is convenient to approximate the first term on the LHS by the first three terms of its Taylor series expansion about the point $\underline{I}_o$. Expanding $H_o(\underline{I})$ about $\underline{I}_o$ gives

$$H_o(\underline{I}) = H_o(\underline{I}_o) + \frac{\partial H_o}{\partial I_x}(I_x - I_{ox}) + \frac{\partial H_o}{\partial I_z}(I_z - I_{oz}) + \qquad (C9)$$

$$\frac{1}{2}\left[\frac{\partial^2 H_o}{\partial I_x^2}(I_x - I_{ox})^2 + 2\,\frac{\partial^2 H_o}{\partial I_z \partial I_x}(I_x - I_{ox})(I_z - I_{oz}) + \frac{\partial^2 H_o}{\partial I_z^2}(I_z - I_{oz})^2\right] + \cdots$$

Using the assumption that $J_2=0$, the coordinate relations (C7), the definitions of the nonlinear frequencies

$$\omega_x(\underline{I}) \equiv \frac{\partial H_o(\underline{I})}{\partial I_x} \qquad (C10)$$

$$\omega_z(\underline{I}) \equiv \frac{\partial H_o(\underline{I})}{\partial I_z}$$

and the definition of the nonlinearity $\Lambda_{\underline{m}}$

$$\Lambda_{\underline{m}} \equiv 2\,m_x m_z \frac{\partial^2 H_o}{\partial I_x \partial I_z} + m_x^2 \frac{\partial^2 H_o}{\partial I_x^2} + m_z^2 \frac{\partial^2 H_o}{\partial I_z^2} \qquad (C11)$$

the Taylor series representation (C9) of H_o can be rewritten

$$H_o(J_1) = H_o(J_1=0) + J_1(\omega_x m_x + \omega_z m_z) + \Lambda_{\underline{m}} J_1^2/2 + \cdots \qquad (C12)$$

Substituting the first three terms of (C12) into (C8), and dropping the irrelevant constant term, the Hamiltonian (C8) becomes approximately

$$K(J_1,\Psi_1) \approx J_1(\omega_x m_x + \omega_z m_z + 2\pi n) + \Lambda_{\underline{m}} J_1^2/2 + 2F_{\underline{m}}(J_1)\cos\Psi_1 \qquad (C13)$$

It is usually possible to neglect the dependence of $F_{\underline{m}}(J_1)$ on J_1 and replace it in (C13) with its constant value $F_{\underline{m}}(0)$ at $J_1=0$.

$$K(J_1,\Psi_1) \approx J_1(\omega_x m_x + \omega_z m_z + 2\pi n) + \Lambda_{\underline{m}} J_1^2/2 + 2F_{\underline{m}}(0)\cos\Psi_1 \qquad (C14)$$

APPENDIX D: Primary Resonance Characteristics

A method for determining the characteristics of a non-linear resonance in a system of N weakly couple oscillators was developed by Chirikov [7]. This appendix reviews this technique for the case N=2. The beam-beam system under consideration is initially defined by the Hamiltonian

$$H = H_z(z,p_z) + H_x(x,p_x) + \sum_{n=-\infty}^{\infty} \delta(t-n)\,V(x,z) \qquad (D1)$$

where $H_z(z,p_z)$ and $H_x(x,p_x)$ represent the linear betatron oscillators. The third term on the RHS represents the periodic beam-beam kick which couples the two oscillators and provides non-linearity. It is convenient to change to the action-angle variables $\underline{I} = \{I_x, I_z\}$ and $\underline{\theta} = \{\theta_x, \theta_z\}$ defined by the linear oscillations

$$\begin{aligned} x &= (2I_x\beta_x)^{1/2}\cos(\theta_x) \\ p_x &= (2I_x/\beta_x)^{1/2}\sin(\theta_x) \end{aligned} \qquad (D2)$$

$$z = (2I_z\beta_z)^{1/2} \cos(\theta_z)$$
$$p_z = (2I_z/\beta_z)^{1/2} \sin(\theta_z)$$

where β_x and β_z are the beta functions at the interaction point. If the beam-beam term in (D1) is Fourier transformed with respect to θ_x and θ_z, the Hamiltonian becomes (see appendix I for details)

$$H = I_x\omega_{ox} + I_z\omega_{oz} + \sum_{\substack{n=-\infty \\ m_x=1 \\ m_z=-\infty}}^{\infty\ \infty\ \infty} 2F_{m_x m_z}\cos(m_x\theta_x + m_z\theta_z + 2\pi n t) + \sum_{\substack{n=-\infty \\ m_z=1}}^{\infty\ \infty} 2F_{o\,m_z}\cos(m_z\theta_z + 2\pi n t) + \sum_{n=1}^{\infty} 2F_{oo}\cos(2\pi n t) + F_{oo} \qquad (D3)$$

The term F_{oo} is dependent on I_x, I_z but independent of θ_x and θ_z. It is convenient to construct an integrable nonlinear oscillator $H_o(\underline{I})$ by adding the two linear oscillator terms to the F_{oo} term from the perturbation expansion.

$$H_o(\underline{I}) = I_x\omega_{ox} + I_z\omega_{oz} + F_{oo}(\underline{I}) \qquad (D4)$$

The Hamiltonian (D3) is not an integrable system, but a finite portion of its phase space is covered by regular trajectories, i.e. trajectories that are bounded for all time and are characterized by discrete frequency spectra (of phase variables). The behavior of such a system is very complicated and can only be understood by carefully examining the properties of its nonlinear resonances (represented by the Fourier terms of (D3)).

An analysis of a certain nonlinear resonance $\underline{m},n$ usually assumes that all of the other Fourier terms in (D3) can be neglected. The resonance Hamiltonian is then

$$H_{\underline{m},n} = H_o(\underline{I}) + 2F_{\underline{m}}(\underline{I})\cos(m_x\theta_x + m_z\theta_z + 2\pi n t) \qquad (D5)$$

The time derivative of the action from Hamilton's equations is

$$\dot{\underline{I}} = -\frac{\partial H_{\underline{m}}}{\partial \underline{\theta}} = \underline{m}\, 2F_{\underline{m}}(\underline{I})\sin(m_x\theta_x + m_z\theta_z + 2\pi n t) \qquad (D6)$$

Equation (D6) shows that in the action space (I_x,I_z), the motion defined by the Hamiltonian (D5) lies on a line parallel to the vector $\underline{m}$. The frequency of oscillation in action space is determined by the time rate of change of the resonance phase $(m_x\theta_x + m_z\theta_z + 2\pi n t)$.

The resonance system (D5) is said to be "in resonance" if the resonance phase is stationary

$$m_x\dot{\theta}_x + m_z\dot{\theta}_z + 2\pi n = 0 \qquad (D7)$$

Since the phase velocities $\dot{\theta}_x$ and $\dot{\theta}_z$ are roughly equal to

$$\dot{\theta}_x \approx \omega_x(\underline{I}) \equiv \frac{\partial H_o(\underline{I})}{\partial I_x}$$
$$\dot{\theta}_z \approx \omega_z(\underline{I}) \equiv \frac{\partial H_o(\underline{I})}{\partial I_z} \qquad (D8)$$

the resonance condition (D7) can be rewritten

$$m_x\omega_x(\underline{I}) + m_z\omega_z(\underline{I}) + 2\pi n = 0 \qquad (D9)$$

The resonance condition is either satisfied on a curve in the action space or not satisfied at all.

Besides its location and the direction of its resonant oscillation, the nonlinear resonance is characterized by a width in action space and a frequency of small amplitude oscillation. To find the resonance width and frequency, a coordinate transformation is made to new variables (J_1,Ψ_1) and (J_2,Ψ_2). Since the system (D5) is integrable, new variables exist for which the Hamiltonian reduces to one degree of freedom. We thus choose the new variables in such a way that one of the new actions, J_2, is an invariant, i.e. such that Ψ_2 does not appear in the Hamiltonian. This coordinate transformation is performed in detail in appendix C. The result is the new Hamiltonian (C8)

$$K(\underline{J},\Psi_1) = H_o(\underline{J}) + 2F_{\underline{m}}(\underline{J})\cos\Psi_1 + J_1 2\pi n \qquad (D10)$$

Two approximations are now made. Firstly, $H_o(\underline{J})$ is replaced by the first three terms of its Taylor series expansion about $\underline{J}=0$ and secondly, $F_{\underline{m}}(\underline{J})$ is replaced by its value $F_{\underline{m}}(0)$ at $\underline{J}=0$. The final result is (C14)

$$K(J_1,\Psi_1) \approx J_1(\omega_x m_x + \omega_z m_z + 2\pi n) + \Lambda_{\underline{m}} J_1^2/2 + 2F_{\underline{m}}(0)\cos\Psi_1 \qquad (D11)$$

where $$J_2 \propto [m_x(I_{oz}-I_z) - m_z(I_{ox}-I_x)] = 0 \qquad (D12)$$

$$J_1 = (I_x-I_{ox})/m_x = (I_z-I_{oz})/m_z \qquad (D13)$$

$$\Psi_1 = m_x\theta_x + m_z\theta_z + 2\pi nt \qquad (D14)$$

and the nonlinearity $\Lambda_{\underline{m}}$ of the $\underline{m}$th resonance is

$$\Lambda_{\underline{m}} \equiv 2\, m_x m_z \frac{\partial^2 H_o}{\partial I_x \partial I_z} + m_x{}^2 \frac{\partial^2 H_o}{\partial I_x{}^2} + m_z{}^2 \frac{\partial^2 H_o}{\partial I_z{}^2} \qquad (D15)$$

The point $\underline{I}_o$ is an arbitrary point in action space. However, since $H_o(\underline{J})$ in (D11) has been approximated by its values close to $\underline{I}_o$, it is necessary to choose $\underline{I}_o$ in such a way that it is close to the initial conditions of the system and such that (D12) is satisfied. Since we are interested here in the characteristics of the $\underline{m}$th resonance, it is natural to choose $\underline{I}_o$ on the resonance line, i.e. such that the resonance condition

$$m_x\omega_x(\underline{I}_o) + m_z\omega_z(\underline{I}_o) + 2\pi n = 0 \qquad (D16)$$

is satisfied. With this choice of $\underline{I}_o$, the Hamiltonian (D11) reduces to the pendulum Hamiltonian

$$K(J_1,\Psi_1) \approx \Lambda_{\underline{m}} J_1{}^2/2 + 2F_{\underline{m}}(0) \cos \Psi_1 \qquad (D17)$$

The small amplitude frequency of the pendulum corresponds to the small amplitude frequency $\omega_{\underline{m}}$ of the resonant oscillation

$$\omega_{\underline{m}} = \sqrt{|2\, F_{\underline{m}}\, \Lambda_{\underline{m}}|} \qquad (D18)$$

The width ΔJ_1 of the resonance corresponds to the pendulum's separatrix width (the full width)

$$\Delta J_1 = 4\sqrt{|2\, F_{\underline{m}}/\Lambda_{\underline{m}}|} \qquad (D19)$$

or, in the original action coordinates, from (D13)

$$\Delta \underline{I} = \underline{m}\, \Delta J_1 \qquad (D20)$$

APPENDIX E: Multiplets and Sidebands

Coupling between the synchrotron and betatron oscillations can result in a low frequency modulation of some parameter in the beam-beam Hamiltonian. This modulation causes each primary beam-beam resonance to split into a multiplet of sideband resonances. Several different types of coupling are possible. If there is non-zero dispersion at the interaction points, the center of the opposing beam appears to sway back and forth with the energy oscillations. If the machine chromaticity is non-zero, the machine tunes oscillate. A sharp dip in the beta-function at the interaction points can create a modulation of the overall beam-beam force or, again, oscillations of the betatron tunes. Although the sources of modulation are diverse, the ways in which they ultimately affect particle motion are very similar. The simplest and probably most significant is tune modulation. In this appendix, the characteristics of the sideband multiplets (the sideband widths, spacings, and frequencies, as well as the full multiplet width), are calculated for the case in which the betatron tune ω_o is forced to oscillate slowly with frequency Ω and amplitude M about some average value $\overline{\omega}_o$.

We start with the 2.5 degree of freedom Hamiltonian for a single primary resonance $\underline{m}$.

$$H_{\underline{m},n}(\underline{I},\underline{\theta}) = H_o(\underline{I}) + 2\, F_{\underline{m}}(0) \cos(\underline{m}\cdot\underline{\theta} + 2\pi nt) \qquad (E1)$$

It can be reduced (approximately) to a 1.5 degree of freedom Hamiltonian (see (D20), appendix D)

$$K(J_1,\Psi_1) \approx J_1(\underline{m}\cdot\underline{\omega}_o + 2\pi n) + \Lambda_{\underline{m}} J_1{}^2/2 + 2F_{\underline{m}}(0) \cos \Psi_1 \qquad (E2)$$

where $$J_1 = (I_x-I_{ox})/m_x = (I_z-I_{oz})/m_z \qquad (E3)$$

$$\Psi_1 = \underline{m}\cdot\underline{\theta} + 2\pi nt \qquad (E4)$$

and the nonlinearity $\Lambda_{\underline{m}}$ of the $\underline{m}$th resonance is defined by

$$\Lambda_{\underline{m}} \equiv 2\, m_x m_z \frac{\partial^2 H_o}{\partial I_x \partial I_z} + m_x{}^2 \frac{\partial^2 H_o}{\partial I_x{}^2} + m_z{}^2 \frac{\partial^2 H_o}{\partial I_z{}^2} \qquad (E5)$$

The constant $F_{\underline{m}}(0)$ is the value of $F_{\underline{m}}(\underline{I})$ at the reference point $\underline{I}_o$ used to define

$J_1=0$. The first term in (E2) would normally be zero since $\underline{I}_0$ is usually taken to be on the resonance line

$$\underline{m}\cdot\underline{\omega}_0(\underline{I}_0) + 2\pi n = 0 \qquad \text{(E6)}$$

We now introduce the modulation. Coupling to the synchrotron motion can cause the betatron tunes to oscillate slowly. If the synchrotron frequency is Ω, and if the amplitudes of the vertical and horizontal tune modulations are M_Z and M_X, then the tunes $\underline{\omega}_0$ can be expressed as

$$\underline{\omega}_0(\underline{I}, t) = \overline{\underline{\omega}}_0(\underline{I}) + \underline{M}\cos\Omega t \qquad \text{(E7)}$$

where $\underline{M} = (M_X, M_Z)$ and $\overline{\underline{\omega}}_0$ is the average vector tune. The action $\underline{I}_0$ now satisfies a modified resonance condition

$$\underline{m}\cdot\overline{\underline{\omega}}_0(\underline{I}) + 2\pi n = 0 \qquad \text{(E8)}$$

and (E2) becomes

$$K(J_1,\Psi_1) = J_1\,\underline{m}\cdot\underline{M}\cos\Omega t + \Lambda_{\underline{m}}J_1^2/2 + 2F_{\underline{m}}(0)\cos\Psi_1 \qquad \text{(E9)}$$

The resonance phase Ψ_1 changes in time at the rate

$$\dot{\Psi}_1 = \partial K/\partial J_1 = \Lambda_{\underline{m}}J_1 + \omega_M\cos\Omega t \qquad \text{(E10)}$$

where $\omega_M \equiv \underline{m}\cdot\underline{M}$. The phase itself may be expressed as

$$\Psi_1 = \Psi_a + (\omega_M/\Omega)\sin\Omega t \qquad \text{(E11)}$$

where
$$\Psi_a \equiv \int_0^t \Lambda_{\underline{m}}J_1(t')\,dt' \qquad \text{(E12)}$$

We now make a coordinate change in which the phase Ψ_1 is replaced by the average phase Ψ_a. We use the generating function

$$G(J_a,\Psi_1) = J_a\Psi_1 - \frac{J_a\,\omega_M}{\Omega}\sin\Omega t \qquad \text{(E13)}$$

which gives
$$J_1 = \partial G/\partial\Psi_1 = J_a$$

$$\Psi_a = \partial G/\partial J_a = \Psi_1 - \frac{\omega_M}{\Omega}\sin\Omega t \qquad \text{(E14)}$$

$$K'(J_a,\Psi_a) = K(J_1,\Psi_1) + \partial G/\partial t = K(J_1,\Psi_1) - J_a\,\omega_M\cos\Omega t \qquad \text{(E15)}$$

In these coordinates, the Hamiltonian (E9) becomes

$$K'(J_a,\Psi_a) = \Lambda_{\underline{m}}J_a^2/2 + 2F_{\underline{m}}(0)\cos\left[\Psi_a + \frac{\omega_M}{\Omega}\sin\Omega t\right] \qquad \text{(E16)}$$

Using the Bessel function identity

$$\cos(A + B\sin\theta) = \sum_{\ell=-\infty}^{\infty} J_\ell(B)\cos(A+\ell\theta) \qquad \text{(E17)}$$

and putting J_1 back in place of J_a, equation (14) can be rewritten

$$K'(J_1,\Psi_a) = \Lambda_{\underline{m}}J_1^2/2 + 2F_{\underline{m}}(0)\sum_{\ell=-\infty}^{\infty} J_\ell(\omega_M/\Omega)\cos(\Psi_a + \ell\Omega t) \qquad \text{(E18)}$$

Sideband Characteristics

In general, from (E3),

$$\Delta I_X = m_X\,|\Delta J_1|$$
$$\Delta I_Z = m_Z\,|\Delta J_1| \qquad \text{(E19)}$$

Sideband Spacing

The sidebands are located in action space by the resonance conditions for the Hamiltonian (E18)

$$\dot{\Psi}_a + \ell\,\Omega = 0$$

or from (E12), $$\Lambda_{\underline{m}}J_1 + \ell\,\Omega = 0 \qquad \text{(E20)}$$

The separation $\Delta^S J_1$ between neighboring sidebands (represented by consecutive values of ℓ) is given directly by (E20)

$$\Delta^S J_1 = \Omega/\Lambda_{\underline{m}} \qquad \text{(E21)}$$

Sideband Width

The Hamiltonian for a single sideband can be obtained by selecting only one term from the sum in (E18)

$$K'(J_1,\Psi_a) = \Lambda_m J_1^2/2 + 2 F_m(0) \; J_\ell(\omega_M/\Omega) \cos(\Psi_a + \ell\Omega t) \qquad (E22)$$

This is the Hamiltonian for the simple pendulum. The width of the sideband $\Delta^W J_1$ is equal to the width of the pendulum separatrix

$$\Delta^W J_1 = 4\sqrt{|2 F_m(J_0) \; J_\ell(\omega_M/\Omega) / \Lambda_m|} \qquad (E23)$$

Unfortunately, $J_\ell(\omega_M/\Omega)$ depends on the particular sideband ℓ, so different sidebands in general have different widths. There is, however, an asymptotic approximation to $J_\ell(x)$ in the limit $x \to \infty$:

$$J_\ell(x) \approx \sqrt{2/(\pi x)} \; \cos(x - \ell\pi/2 - \pi/4) \qquad (E24)$$

The rms magnitude of $J_\ell(x)$ for sidebands inside the multiplet can thus be estimated

$$\langle J_\ell(x) \rangle \approx (\pi x)^{-1} \qquad (E25)$$

or with $x = \omega_M/\Omega$, when $|\ell| < |\omega_M/\Omega|$

$$\langle J_\ell(\omega_M/\Omega) \rangle \approx \sqrt{|\Omega/\pi\omega_M|} \qquad (E26)$$

For $|\ell| > |\omega_M/\Omega|$, $\langle J_\ell \rangle$ falls of exponentially fast with $|\ell|$. Thus, only the sidebands with $|\ell| < |\omega_M/\Omega|$ are of substantial size. The modulation thus causes the primary resonance to split into a multiplet of $2\omega_M/\Omega$ sidebands. The average widths of the multiplet sidebands can be obtained by substituting (E26) for $J_\ell(\omega_M/\Omega)$ in (E23)

$$\langle \Delta^W J_1 \rangle = 4 \left| \frac{2F_m}{\Lambda_m} \right|^{1/2} \left| \frac{\Omega}{\pi\omega_M} \right|^{1/4} \qquad (E27)$$

which can be written

$$\langle \Delta^W J_1 \rangle = \Delta J_1 \left| \frac{\Omega}{\pi\omega_M} \right|^{1/4} \qquad (E28)$$

where ΔJ_1 is the width (D19) of the primary resonance. The sideband width is evidently only very weakly dependent on the characteristics of the modulation, Ω and M. In a typical e^+-e^- machine, $\Omega \approx .1$, and $\omega_M \approx .1$. Then $(\Omega/\omega_M)^{1/4} \approx 1$ so that the sidebands are generally about $\pi^{-1/4} = .75$ the width of the primary resonance.

MULTIPLET WIDTH

The number of sidebands in the multiplet is equal to twice the value of ℓ above which the magnitude of the Bessel functions begins to fall off exponentially.

$$\text{Number of sidebands} = \quad 2\,\omega_M/\Omega \qquad (E29)$$

The width of the multiplet in J_1 is given, then, by

$$\Delta^M J_1 = \text{number of sidebands} \times \Delta^S I_m$$

$$\Delta^M J_1 = 2\,\omega_M / \Lambda_m \qquad (E30)$$

APPENDIX F: Transport Regime Thresholds

There are two characteristic transport thresholds: the resonance overlap threshold and the trapping threshold. These two thresholds divide parameter space into three regimes:

a) the stable or regular regime in which no transport takes place,
b) the quasilinear regime in which particles diffuse at the quasilinear diffusion rate, and
c) the adiabatic regime where the diffusion is adiabatic.

We calculate here the two threshold conditions separating these regimes.

SIDEBAND OVERLAP THRESHOLD

The sideband overlap threshold determines the tuneshift above which the sidebands of a particular resonance will overlap at a particular point in action space. The criterion for sideband resonance overlap is that the ratio of sideband width to spacing must be greater than $2/\pi$. From Appendix E, equations (E27) and (E21), the sideband average widths and spacings are given by

$$\langle \Delta^W J_1 \rangle = 4 \left| \frac{2F_{\underline{m}}}{\Lambda_{\underline{m}}} \right|^{1/2} \left| \frac{\Omega}{\pi \omega_M} \right|^{1/4}$$

$$\Delta^S J_1 = \Omega \; / \; \Lambda_{\underline{m}}$$

The sideband overlap condition, as shown by Chirikov [7], is the condition that the ratio of sideband width to sideband spacing be greater than $2/\pi$.

$$\frac{\langle \Delta^W J_1 \rangle}{\Delta^S J_1} = 4/\Omega \; (2F_{\underline{m}}\Lambda_{\underline{m}})^{1/2} \, (\Omega/\pi\omega_M)^{1/4} > \frac{2}{\pi} \qquad \text{(F1)}$$

or substituting $\Omega = 2\pi/P$

$$2P/\pi \; (2F_{\underline{m}}\Lambda_{\underline{m}})^{1/2} \, (2/P\,\omega_M)^{1/4} > \frac{2}{\pi}$$

$$P \, (2F_{\underline{m}}\Lambda_{\underline{m}})^{1/2} \, (2/P\,\omega_M)^{1/4} > 1 \qquad \text{(F2)}$$

Raising to the fourth power gives

$$2P^3 \, (2F_{\underline{m}}\Lambda_{\underline{m}})^2 \, / \, \omega_M > 1 \qquad \text{(F3)}$$

or finally,

$$(2F_{\underline{m}}\Lambda_{\underline{m}})^2 > \frac{\omega_M}{2\,P^3} \qquad \text{(F4)}$$

The most important feature of this result is the dependence on modulation period P. Sideband overlap, and thus stochastic diffusion, is more likely to occur at low synchrotron frequencies than high.

TRAPPING THRESHOLD

The trapping threshold defines the boundary between the quasilinear regime and the adiabatic regime. It is defined by the condition that particles can be trapped in the primary resonance and dragged along with it as it sways back and forth in action space. In order to trap a particle, a resonance must be able to push a particle through action space at least as fast as the resonance itself is moving through the the action space. The rate $\dot{J}_r$ at which the primary resonance is moving through action space is given by...

$$\dot{J}_r = \frac{\partial J_1}{\partial \dot{\psi}_1} \frac{\partial \dot{\psi}_1}{\partial t} \qquad \text{(F5)}$$

Now, since

$$\frac{\partial \dot{\psi}_1}{\partial J_1} = \Lambda_{\underline{m}} \qquad \text{(F6)}$$

$$\frac{\partial \dot{\psi}_1}{\partial t} = \frac{\partial}{\partial t} \left(\underline{m}\cdot\underline{\theta} + 2\pi n t \right)$$

$$\frac{\partial \dot{\psi}_1}{\partial t} \approx \frac{\partial}{\partial t} \left(\underline{m}\cdot\underline{\bar{\omega}}_o + \underline{m}\cdot\underline{M} \cos \Omega t + 2\pi n t \right)$$

$$\approx - \omega_M \, \Omega \sin \Omega t \qquad \text{(F7)}$$

where $\omega_M = \underline{m}\cdot\underline{M}$. Then

$$\dot{I}_r = \frac{-\omega_M \Omega}{\Lambda_{\underline{m}}} \sin \Omega t \qquad \text{(F8)}$$

The maximum rate at which the primary resonance is moving through $I_{\underline{m}}$ space is then given by...

$$\max \left(\dot{I}_r \right) = \frac{\omega_M \, \Omega}{\Lambda_{\underline{m}}} \qquad \text{(F9)}$$

The trapping threshold is defined by the condition that this rate be equal to the maximum rate at which the resonance can push a particle. For the Hamiltonian

$$K(J_1,\Psi_1) = \Lambda_m J_1^2/2 + 2 F_m(0) \cos \Psi_1 \qquad (F10)$$

the rate $\dot{J}_1$ at which the resonance pushes a phase particle is given by..

$$\dot{J}_1 = -\frac{\partial H_m}{\partial \Psi_1} = 2 F_m \sin \Psi_1 \qquad (F11)$$

with

$$\max \dot{J}_1 = 2 F_m \qquad (F12)$$

The trapping threshold is then obtained by equating (F9) to (F12). Trapping occurs if

$$|2 F_m| > \left|\frac{\omega_M \Omega}{\Lambda_m}\right|$$

or

$$|2 F_m \Lambda_m| > |\omega_M \Omega| \qquad (F13)$$

RELATIONSHIPS BETWEEN QUASILINEAR AND ADIABATIC REGIMES

Its useful to express both (F4) and (F13) in terms of the three characteristic frequencies: the libration frequency of the primary resonance ω_m, the modulation frquency Ω, and the multiplet half-width ω_M in $\dot{\Psi}_1$

$$\omega_m \equiv \sqrt{|2 F_m \Lambda_m|}$$
$$\omega_M \equiv |m \cdot M|$$

Then the condition for sideband overlap (F3) is

$$\omega_m^4 > \frac{\omega_M \Omega^3}{2 (2\pi)^3} \qquad (F14)$$

and the adiabaticity condition (F13) is

$$\omega_m^2 > \omega_M \Omega \qquad (F15)$$

These conditions are valid as long as there is more than one sideband in the multiplet. We thus have an auxilliary validity condition

$$\omega_M > \Omega \qquad (F16)$$

Each of the conditions (F14), (F15), and (F16) defines a surface in the three dimensional space spanned by the coordinates ω_m^2, ω_M, and Ω.

APPENDIX G: Quasilinear Diffusion Rate

In a multiplet of overlapping sidebands, there are two diffusion regimes, the quasilinear regime and the adiabatic or trapping regime. In this section the diffusion rate in quasilinear regime is calculated.

Quasilinear Diffusion

In this regime, the primary resonance is sweeping back and forth slowly enough that the sidebands overlap, but not so slowly that particles become trapped in the primary resonance.

Diffusion in this parameter regime corresponds to the so-called "quasilinear diffusion" which is used extensively in the theory of particle motion in turbulent wave fields. The validity of quasilinear theory depends on the satisfaction of two conditions: the first is the "free particle" condition which requires that the particle trajectory deviate insignificantly from its free particle trajectory during one correlation time of the field. The second is the "random phase" condition which requires that the phases of the different waves affecting the particle motion be uncorrelated. The first of these conditions corresponds to equation (F19) for the threshold between the quasilinear and adiabatic regimes, and the second to equation (F18) which defines the threshold for sideband overlap. We derive here the quasilinear diffusion rate for a one dimensional system in which a charged particle is driven by a number of equally spaced (in frequency) electrostatic waves. We assume that the waves all have the same wave number k, but that their phases are random with respect to one another. The wave-particle Hamiltonian is

$$H = p^2/2m + \sum_{n=-\infty}^{\infty} A_n \exp[i(kx-\Omega nt)] \qquad (G1)$$

where the A_n are complex numbers. Quasilinear condition #1 above allows us to assume that the particle's velocity doesn't change much in one correlation time, so the Hamiltonian can be approximated with

$$H \approx vp + \sum_{n=-\infty}^{\infty} A_n \exp[i(kx-\Omega nt)]$$

where v is a constant equal to the initial velocity of the particle. Then

$$x = x_0 + vt$$

and

$$\dot{p} = -\frac{\partial H}{\partial x} = \sum_{n=-\infty}^{\infty} -ik\ A_n\ \exp[i(kx-n\Omega t)]$$

$$\Delta p(t) = \int_0^t dt' \sum_{n=-\infty}^{\infty} -ik\ A_n \exp[i\{k(x_0+vt')-n\Omega t'\}]$$

$$= \sum_{n=-\infty}^{\infty} \frac{-ik\ A_n}{(kv-n\Omega)} \left[\exp[i\{k(x_0+vt)-n\Omega t\}] - \exp[ikx_0] \right]$$

$$\Delta p^2(t) = \sum_{n'=-\infty}^{\infty} \sum_{n''=-\infty}^{\infty} \frac{k^2 A_{n'}}{(kv-n'\Omega)} \left[\exp[i\{k(x_0+vt)-n'\Omega t\}] - \exp[ikx_0] \right] \times \frac{A_{n''}^*}{(kv-n''\Omega)} \left[\exp[-i\{k(x_0+vt)-n''\Omega t\}] - \exp[-ikx_0] \right]$$

We now average over the phases θ_n of $A_n = |A_n| e^{(i\theta_n)}$. Each term in the above sum is a product $(A_{n'})\times(A^*_{n''})$ of two complex numbers $A_{n'}$ and $A_{n''}$. The ensemble over which the average is to be made is the "random phase" ensemble corresponding to the assumption #2 of quasilinear theory. It may be represented by a uniform distribution on an infinite dimensional torus, the coordinates of which are the phases θ_n. The averages of the cross terms are all zero, leaving

$$\langle \Delta p^2(t) \rangle = \sum_{n=-\infty}^{\infty} \frac{k^2 |A_n|^2}{(kv-n\Omega)^2} \left| \exp[i\{k(x_0+vt)-n\Omega t\}] - \exp[ikx_0] \right|^2$$

The product of exponentials is

$$\left| \exp[i\{k(x_0+vt)-n\Omega t\}] - \exp[ikx_0] \right|^2 = 1 + 1 - e^{-i(kv-n\Omega)t} - e^{i(kv-n\Omega)t}$$

$$= 4 \sin^2 \{(kv-n\Omega)t/2\}$$

The variance thus reduces to

$$\langle \Delta p^2(t) \rangle = k^2\, 4 \sum_{n=-\infty}^{\infty} |A_n|^2 \frac{\sin^2 \{(kv-n\Omega)t/2\}}{(kv-n\Omega)^2}$$

If the spectral density $S = |A_n|^2/\Omega$ is held to a constant function of frequency $\omega=n\Omega$ while the frequency spacing Ω is decreased to zero, the above sum converges to an integral over ω

$$\langle \Delta p^2(t) \rangle = k^2\, 4 \int_{-\infty}^{\infty} d\omega\ S\ \frac{\sin^2 \{(kv-\omega)t/2\}}{(kv-\omega)^2}$$

$$= k^2\, 4\, S\, \pi t/2$$

The quasilinear diffusion rate is then given by

$$D \equiv \langle \Delta p^2(t) \rangle / 2t = k^2\, S\, \pi \qquad \text{(G2)}$$

The quasilinear diffusion rate is remarkably simple since it depends only on the value of the spectral density at the resonant frequency (where $\omega=kv_p$ with v_p the particle velocity). It is independent of the frequency spacing between waves, or the width of the full frequency spectrum.

Application to Overlapping Sideband Multiplets

The beam-beam system with tune modulation is defined by (E18)

$$K'(J_1,\Psi_a) = \Lambda_{\underline{m}}\, J_1^2/2 + 2\, F_{\underline{m}}(0) \sum_{\ell=-\infty}^{\infty} J_\ell(\omega_M/\Omega) \cos(\Psi_a + \ell\Omega t)$$

Comparing to the wave-particle Hamiltonian (G1), k=1 and the wave spectral energy density corresponds to

$$S = \frac{(2F_{\underline{m}}\langle J_\ell \rangle)^2}{\Omega}$$

Using this and (E26)

$$\langle J_\ell \rangle = |\Omega/\pi\omega_M|^{1/2}$$

the beam-beam quasilinear diffusion rate is

$$D_{ql} = |(2F_{\underline{m}})^2 / \omega_M| \qquad \text{(G3)}$$

This is the rate at which the random variable J_1 diffuses. The rates of diffusion of the two amplitudes a_x and a_z are obtained by first changing to the action variables I_x and I_z by multiplying (G3) by m_x^2 and m_z^2 respectively, and then to the amplitudes by multiplying by the squares of the appropriate Jacobians.

$$D(a_x) = \left[m_x \frac{\partial a_x}{\partial I_x} \right]^2 D_{ql} = \left[\frac{m_x \xi_x}{a_x \sigma_x} \right]^2 D_{ql}$$

$$D(a_z) = \left[m_z \frac{\partial a_x}{\partial I_z} \right]^2 D_{ql} = \left[\frac{m_z \xi_z}{a_z \sigma_z} \right]^2 D_{ql} \qquad \text{(G4)}$$

The expressions on the right make use of the relation (A9) for the Jacobians.

APPENDIX I: Fourier Transform

The beam-beam Hamiltonian is

$$H = I_x\omega_{ox} + I_z\omega_{oz} + \delta_t\, V(I_x,I_z,\theta_x,\theta_z) \qquad (11)$$

where $\delta_t \equiv \sum_{n=-\infty}^{\infty} \exp(i2\pi nt)$

Since the imaginary part of the nth term in δ_t cancels the imaginary part of the -nth term,

$$\delta_t \equiv \sum_{n=-\infty}^{\infty} \cos 2\pi nt$$

The Fourier transform is defined to be

$$F_{m_x m_z} = \frac{1}{(2\pi)^2}\int_0^{2\pi} d\theta_x \int_0^{2\pi} d\theta_z \exp\{i(m_x\theta_x + m_z\theta_z)\}\, V(I_x,I_z,\theta_x,\theta_z) \qquad (12)$$

For notational convenience, the I_x,I_z dependence on the LHS has not been shown explicitly. Since $V(I_x,I_z,\theta_x,\theta_z)$ is usually even in both θ_x and θ_z, the imaginary part of the exponential factor in the above equation gives no contribution to the integral. Thus

$$F_{m_x m_z} = \frac{1}{(2\pi)^2}\int_0^{2\pi} d\theta_x \int_0^{2\pi} d\theta_z \cos(m_x\theta_x + m_z\theta_z)\, V(I_x,I_z,\theta_x,\theta_z) \qquad (13)$$

The Hamiltonian can now be written

$$H = I_x\omega_{ox} + I_z\omega_{oz} + \sum_{n=-\infty}^{\infty}\cos(2\pi nt) \sum_{\substack{m_x=-\infty\\ m_z=-\infty}}^{\infty} F_{m_x m_z} \exp[-i(m_x\theta_x + m_z\theta_z)]$$

since $V(I_x,I_z,\theta_x,\theta_z)$ is real, the imaginary part of the m_x,m_z term is cancelled by the imaginary part of the $-m_x,-m_z$ term. In fact, since $V(I_x,I_z,\theta_x,\theta_z)$ is usually symmetric with respect to θ_x and θ_z, $F_{mx\ mz}$ is usually real and equal to F_{-mx-mz}. We may therefore halve the number of terms in the above equation. The third term in this equation becomes

$$\sum_{n=-\infty}^{\infty}\cos(2\pi nt)\left[\sum_{\substack{m_x=1\\ m_z=-\infty}}^{\infty} 2F_{m_x m_z}\cos(m_x\theta_x + m_z\theta_z) + F_{oo} + \sum_{m_z=1}^{\infty} 2F_{o\,m_z}\cos(m_z\theta_z)\right]$$

Now $\cos(\alpha)\cos(\beta) = 1/2\,[\cos(\alpha+\beta) + \cos(\alpha-\beta)]$ so that...

$$\cos(2\pi nt)\cos(m_x\theta_x + m_z\theta_z) = 1/2\,[\cos(m_x\theta_x + m_z\theta_z + 2\pi nt) + \cos(m_x\theta_x + m_z\theta_z - 2\pi nt)]$$

Since half of this nth term can be associated with the -nth term, the full Hamiltonian can be rewritten

$$H = I_x\omega_{ox} + I_z\omega_{oz} + \sum_{\substack{n=-\infty\\ m_x=1\\ m_z=-\infty}}^{\infty} 2F_{m_x m_z}\cos(m_x\theta_x + m_z\theta_z + 2\pi nt) + \sum_{\substack{n=-\infty\\ m_z=1}}^{\infty} 2F_{o\,m_z}\cos(m_z\theta_z + 2\pi nt) + \sum_{n=1}^{\infty} 2F_{oo}\cos(2\pi nt) + F_{oo} \qquad (14)$$

Note that if $V(I_x,I_z,\theta_x,\theta_z)=1$, $F_{oo}=1$. On the other hand, if $V(I_x,I_z,\theta_x,\theta_z) = \cos(m_x\theta_x + m_z\theta_z)$, then $F_{mx,mz}=1/2$ and $F_{-mx,-mz}=1/2$ which is taken into account by the factors of 2 in the summation terms.

APPENDIX J: Generating Function

The linear generating function for the transformation is given by

$$G = \underline{I_o}\cdot\underline{\theta} - \underline{J}\cdot\boldsymbol{\mu}\cdot\underline{\theta} + J_1 2\pi nt \qquad (J1)$$

where $\boldsymbol{\mu}$ is a 2x2 tensor of the form

$$\boldsymbol{\mu} \equiv \begin{vmatrix} \mu_{xx} & \mu_{zx} \\ \mu_{xz} & \mu_{zz} \end{vmatrix}$$

The new coordinates are then defined by the relations

$$\Psi_1 \equiv \frac{\partial G}{\partial J_1} \qquad \Psi_2 \equiv \frac{\partial G}{\partial J_2}$$

$$I_x = \frac{\partial G}{\partial \theta_x} \qquad I_z = \frac{\partial G}{\partial \theta_z}$$

and the new Hamiltonian by

$$K(\underline{J}, \underline{\Psi}) = H(\underline{I}, \underline{\theta}) + \partial G/\partial t$$

Rewriting (J1) in terms of its separate components gives

$$G = I_{ox}\theta_x + I_{oz}\theta_z + J_1\mu_{xx}\theta_x + J_1\mu_{zx}\theta_z + J_2\mu_{xz}\theta_x + J_2\mu_{zz}\theta_z + 2\pi nt J_1$$

so...

$$\begin{aligned} \Psi_1 &= \partial G/\partial J_1 = \mu_{xx}\theta_x + \mu_{zx}\theta_z + 2\pi nt \\ \Psi_2 &= \partial G/\partial J_2 = \mu_{xz}\theta_x + \mu_{zz}\theta_z \\ I_x &= \partial G/\partial \theta_x = I_{ox} + J_1\mu_{xx} + J_2\mu_{xz} \\ I_z &= \partial G/\partial \theta_z = I_{oz} + J_1\mu_{zx} + J_2\mu_{zz} \end{aligned} \qquad (J2)$$

Rewritting the last two equations of (J2) two different ways gives

$$\mu_{zx}(I_x - I_{ox}) = J_1\mu_{xx}\mu_{zx} + J_2\mu_{xz}\mu_{zx} \qquad (J3)$$

$$\mu_{xx}(I_z - I_{oz}) = J_1\mu_{zx}\mu_{xx} + J_2\mu_{zz}\mu_{xx} \qquad (J4)$$

and

$$\mu_{zz}(I_x - I_{ox}) = J_1\mu_{xx}\mu_{zz} + J_2\mu_{xz}\mu_{zz} \qquad (J5)$$

$$\mu_{xz}(I_z - I_{oz}) = J_1\mu_{zx}\mu_{xz} + J_2\mu_{zz}\mu_{xz} \qquad (J6)$$

Subtracting (J4) from (J3) and (J6) from (J5) gives

$$J_1 = \frac{\mu_{zz}(I_x - I_{ox}) - \mu_{xz}(I_z - I_{oz})}{\text{Det } \boldsymbol{\mu}} \qquad (J7)$$

$$J_2 = \frac{\mu_{xx}(I_z - I_{oz}) - \mu_{zx}(I_x - I_{ox})}{\text{Det } \boldsymbol{\mu}} \qquad (J8)$$

Now when $J_2 = 0$, from (J5) and (J 6), then

$$(I_x - I_{ox}) = J_1\,\mu_{xx} \qquad (J9)$$

$$(I_z - I_{oz}) = J_1\,\mu_{zx} \qquad (J10)$$

Since we want J_2 to be an invariant , we choose the components of $\boldsymbol{\mu}$ to be such that

$$\Psi_1 = m_x\theta_x + m_z\theta_z + 2\pi nt \qquad (J11)$$

From (J2), this condition is met if $\mu_{xx} = m_x$ and $\mu_{zx} = m_z$. This specification alone (leaving μ_{xz} and μ_{zz} left unspecified) results in the following additional identities:

From (J8),

$$J_2 = \frac{m_x(I_z - I_{oz}) - m_z(I_x - I_{ox})}{\text{Det } \boldsymbol{\mu}} \qquad (J15)$$

and, when $J_2=0$,

$$\begin{aligned} \Delta I_x \equiv (I_x - I_{ox}) &= m_x\,J_1 \\ \Delta I_z \equiv (I_z - I_{oz}) &= m_z\,J_1 \end{aligned} \qquad (J16)$$

Since $\Delta\underline{I}$ is always parallel to the vector $\underline{m}$ and the system is assumed to be initially at $\underline{I}_o$,

$$\frac{\Delta I_x}{\Delta I_z} = \frac{m_x}{m_z}$$

Thus, from (J15), $J_2 = 0$ always.

Note that specification of μ_{xx} and μ_{zx} defines J_2 everywhere, but J_1 only on the line $J_2 = 0$. However, since the system is confined for all time to this line, knowledge about J_1 is not needed for $J_2 \neq 0$.

REFERENCES

1. J.L. Tennyson, "The Dynamics of the Beam-Beam Interaction", in **Physics of High Energy Particle Accelerators,** ed.s R.A. Carrigan, F.R. Huson, M. Month; AIP Conference Proceedings No. 87, AIP Press, New York (1982).
2. F.M. Izrailev, S.I. Misnev, G.M. Tumaikin, "Numerical Studies of Stochasticity Limit in Colliding Beams (one dimensional model)", INP preprint No. 77-43, Institute of Nuclear Physics, Novosibirsk (1977); F.M. Izrailev, S.I. Misnev, G.M. Tumaikin and I.B. Vasserman, Proc. Xth Int. Conf. on High Energy Acc., Serpukhov (1977) v. 11, p.302.
3. J.L. Tennyson, "The Instability Threshold for Bunched Beams in Isabelle", in **Nonlinear Dynamics and the Beam-Beam Interaction,** ed.s M. Month and J.C. Herrera; AIP Conference Proceedings No. 57, AIP Press, New York (1979).
4. F.M. Izrailev and I.B. Vasserman, "The Influence of Different Types of Modulations on a Decrease of the Stochasticity Limit in Beam-Beam Effects", INP preprint No. 81-60, Institute of Nuclear Physics, Novosibirsk (1981).
5. L.R. Evans, "The Beam-Beam Interaction", internal report CERN SPS/83-38 (DI-MST) (1983).
6. A.L. Gerasimov, F.M. Izrailev, J.L. Tennyson, "A Description of Nonlinear Resonances for Colliding Beams with Large Aspect Ratios", INP preprint No. 86-98 (in Russian), Institute of Nuclear Physics, Novosibirsk (1986).
7. B.V. Chirikov, "Universal Instability of Many Dimensional Oscillator Systems", Physics Reports **52** 263 (1979).
8. H. Wiedemann, "Experiments on the Beam-Beam Effect in e^+e^- Storage Rings", in **Nonlinear Dynamics and the Beam-Beam Interaction,** ed.s M. Month and J.C. Herrera; AIP Conference Proceedings No. 57, AIP Press, New York (1979).

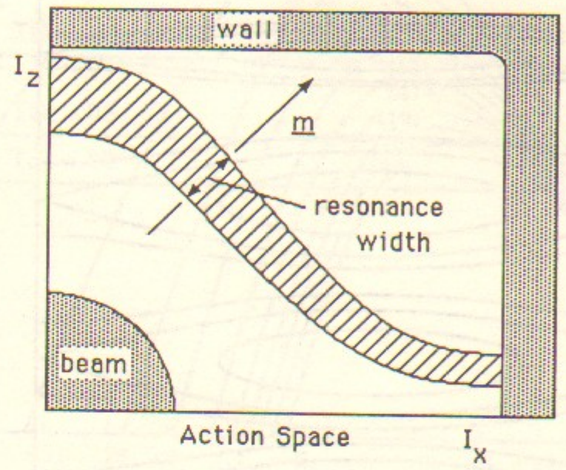

Figure 1. Nonlinear Resonance in the Amplitude Plane

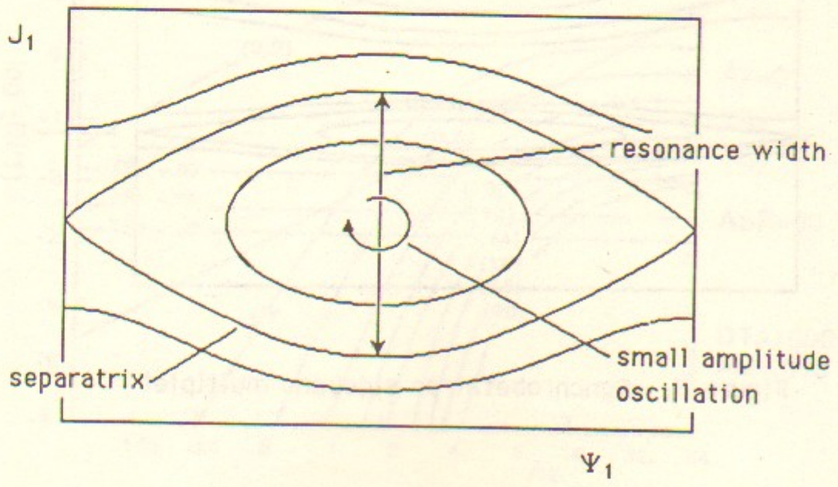

Figure 2. Nonlinear Resonance in Phase Space

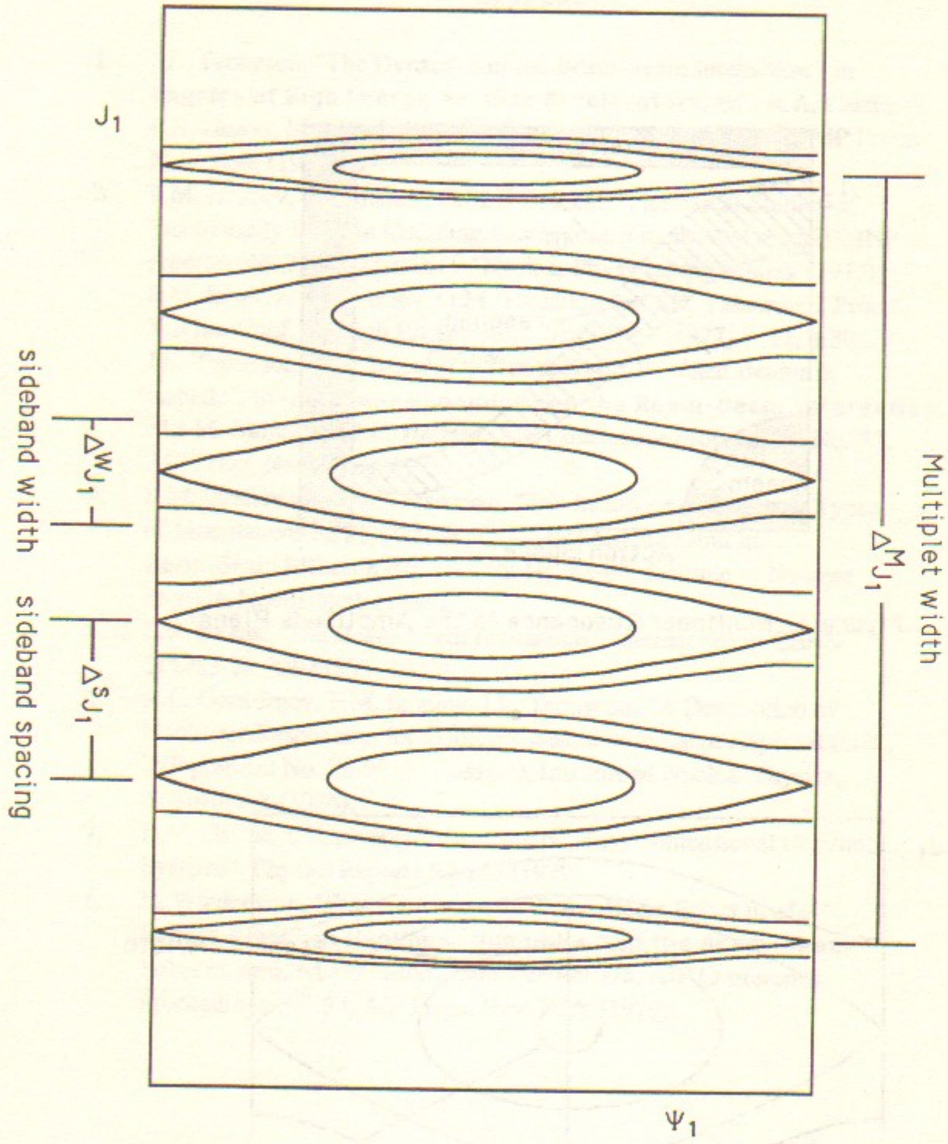

Figure 3: Synchrobetatron sideband multiplet

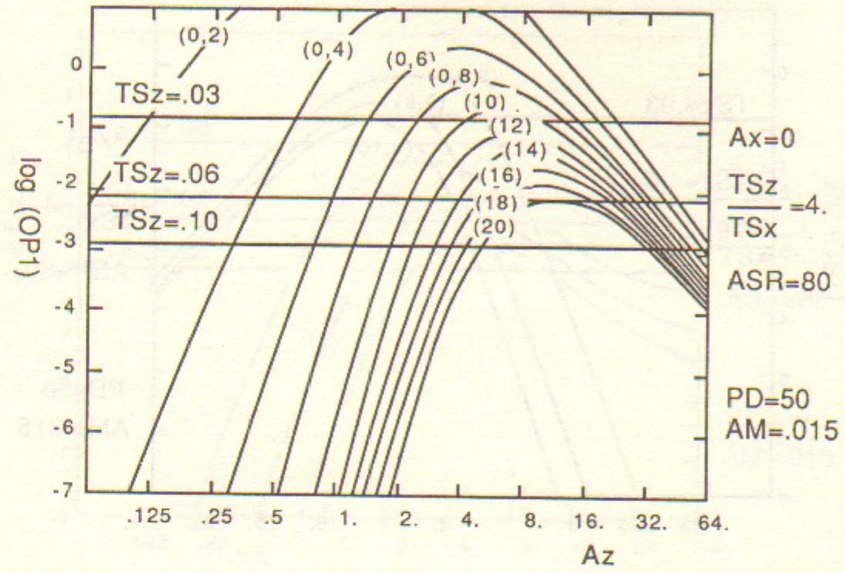

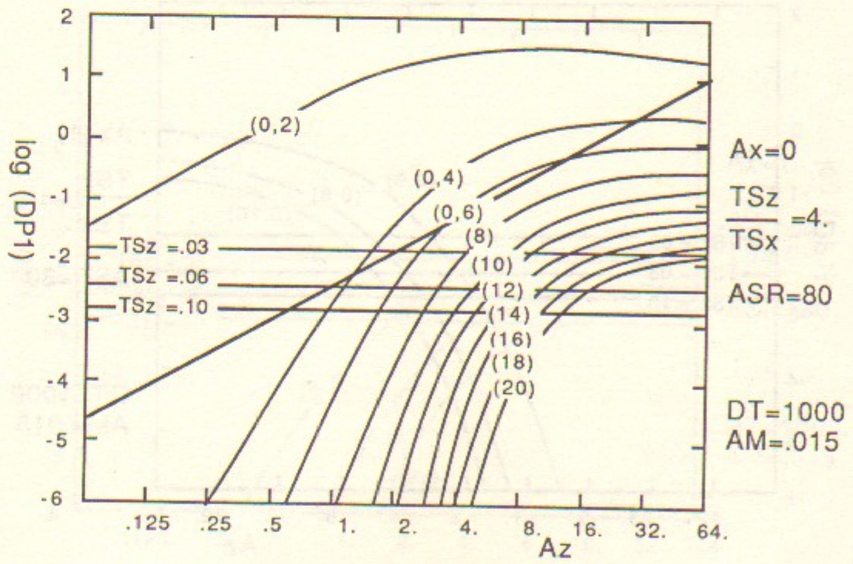

Figure 4: Thresholds for parametric resonances at $A_x = 0$.

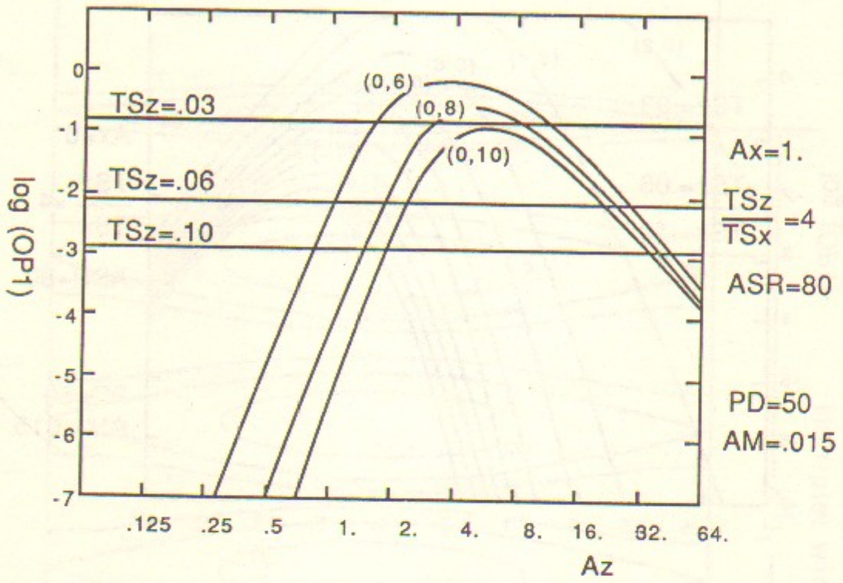

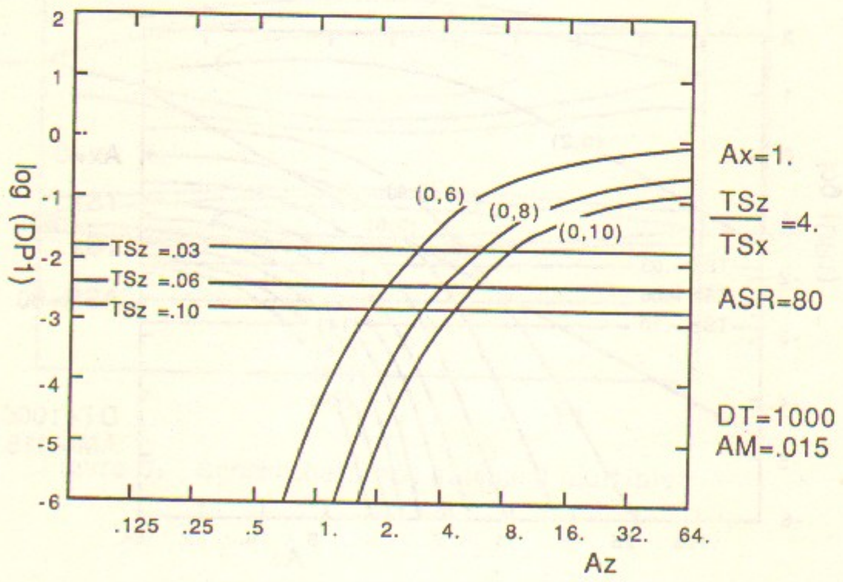

Figure 5a.1: Thresholds at Ax=1

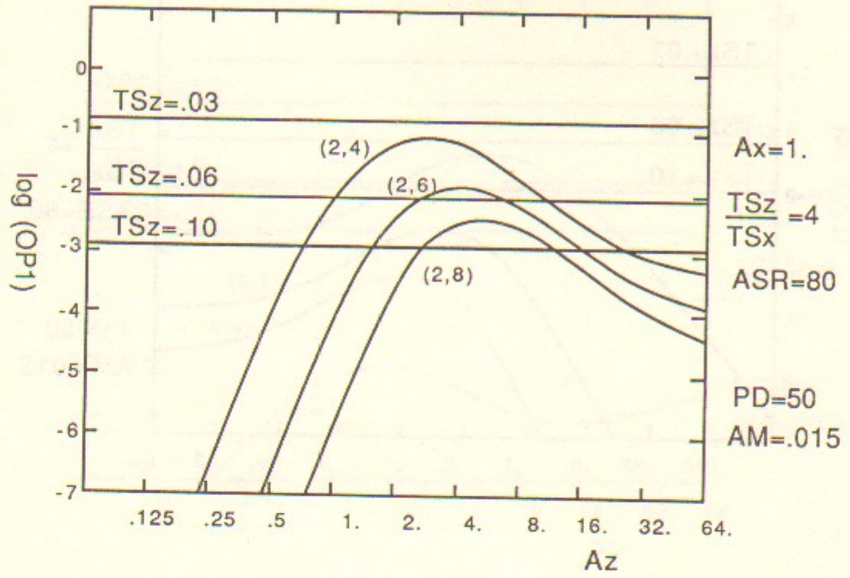

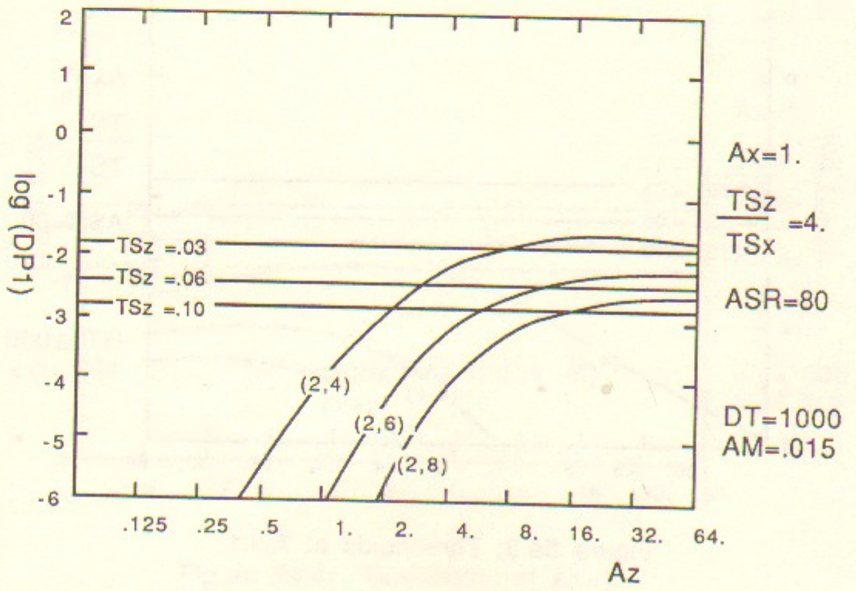

Figure 5a.2: Thresholds at Ax=1

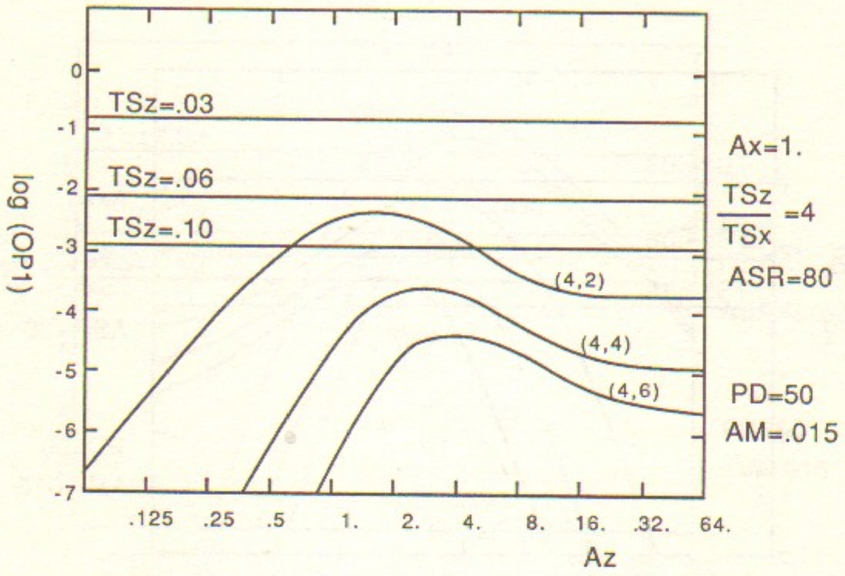

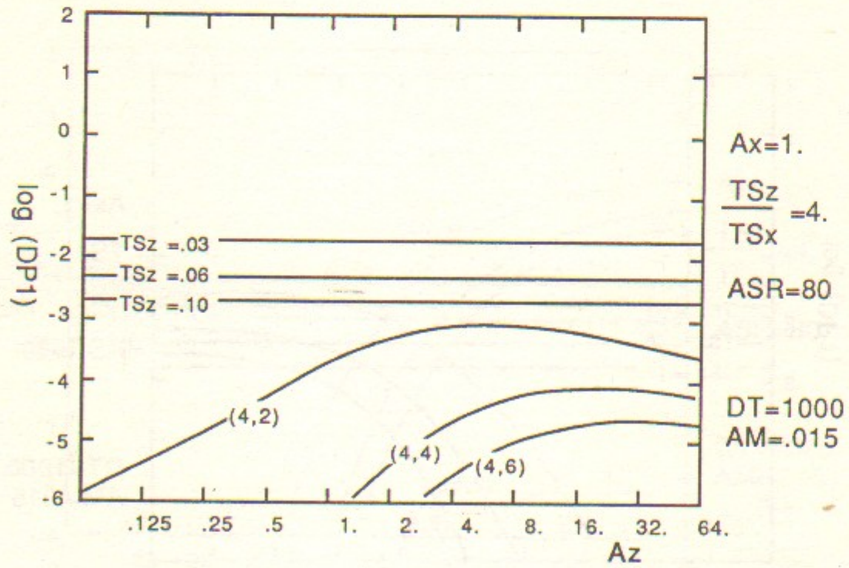

Figure 5a.3: Thresholds at Ax=1

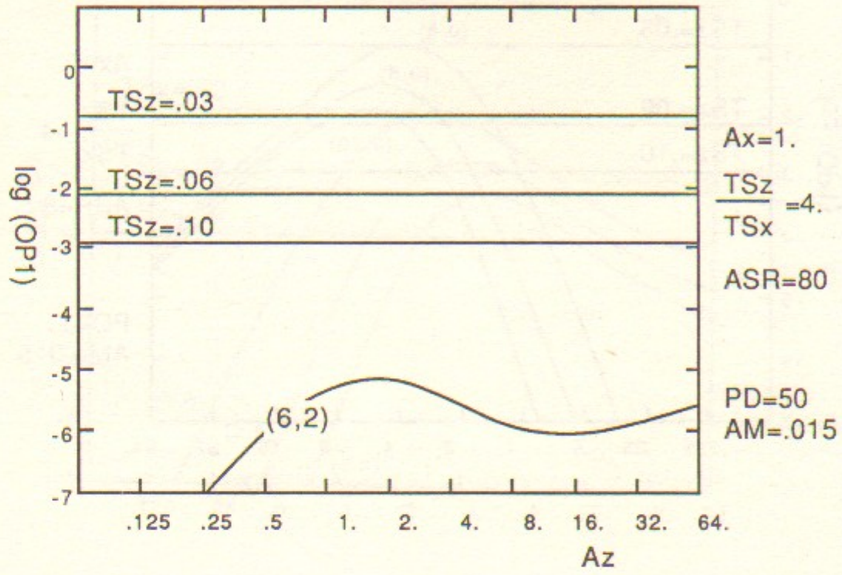

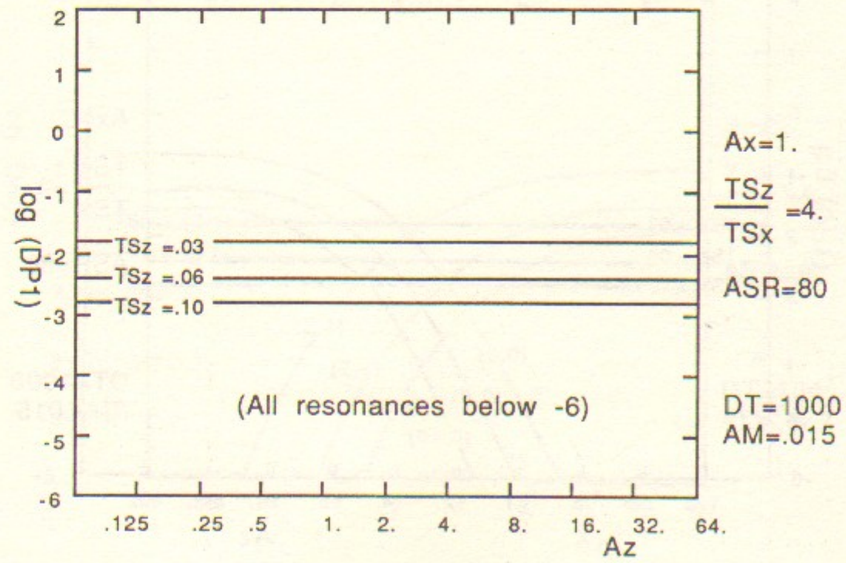

Figure 5a.4: Thresholds at Ax=1

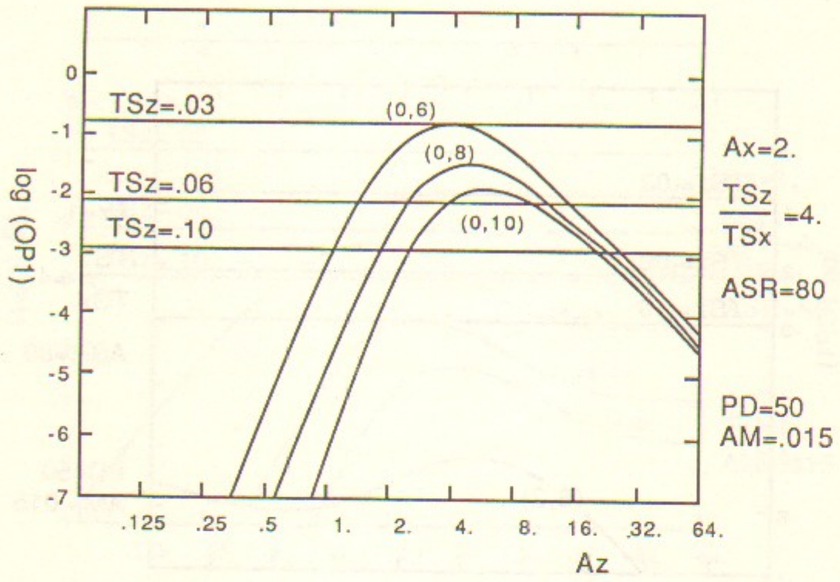

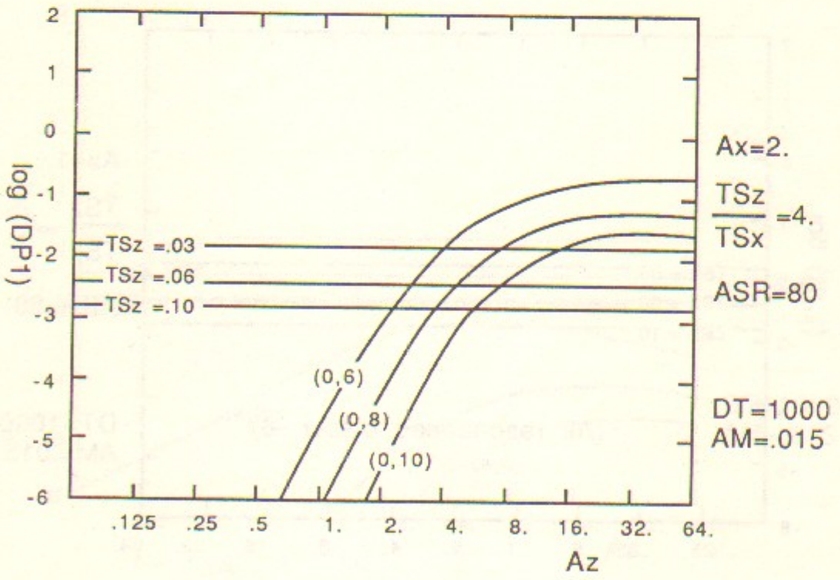

Figure 5b.1 Thresholds at Ax=2

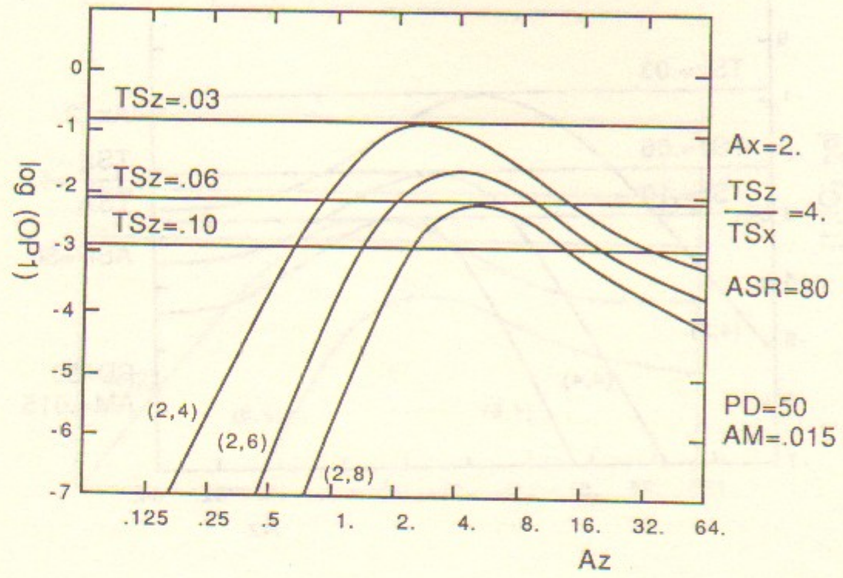

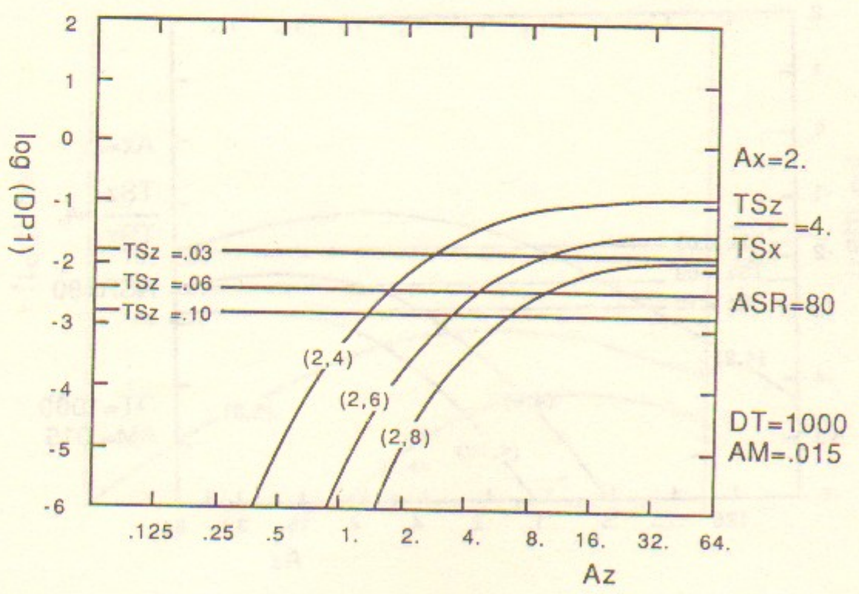

Figure 5b.2 Thresholds at Ax=2

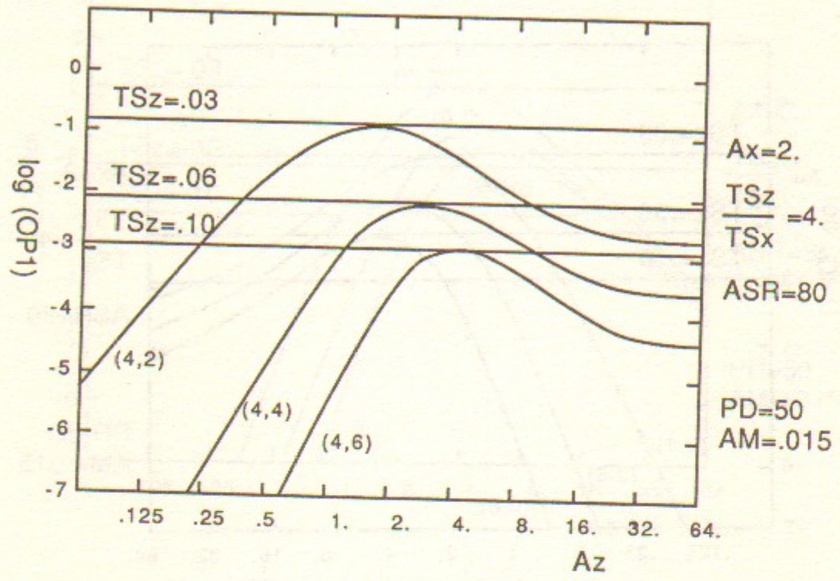

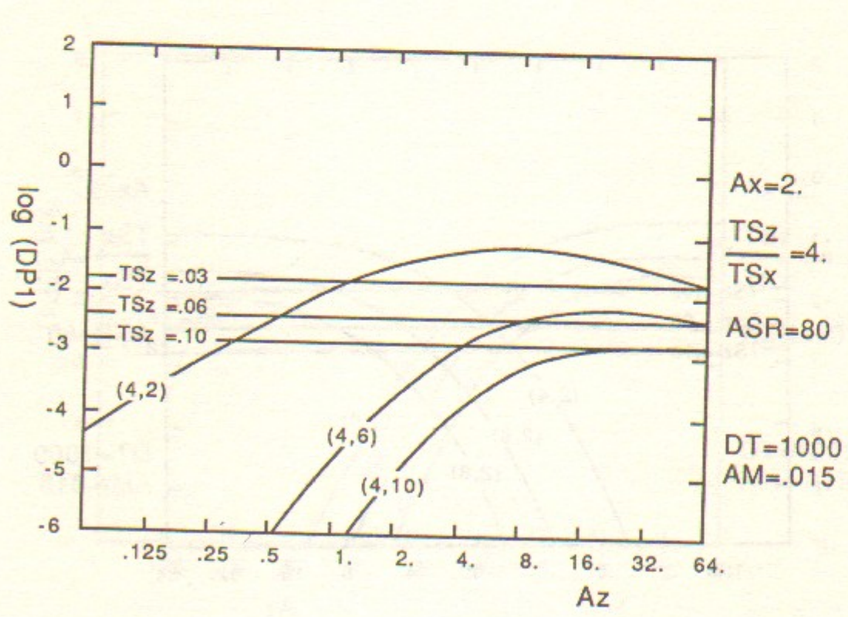

Figure 5b.3 Thresholds at Ax=2

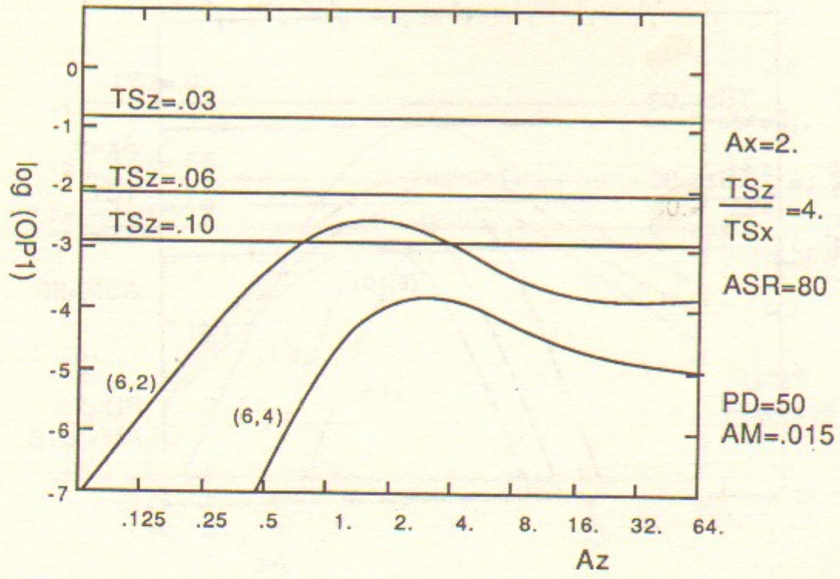

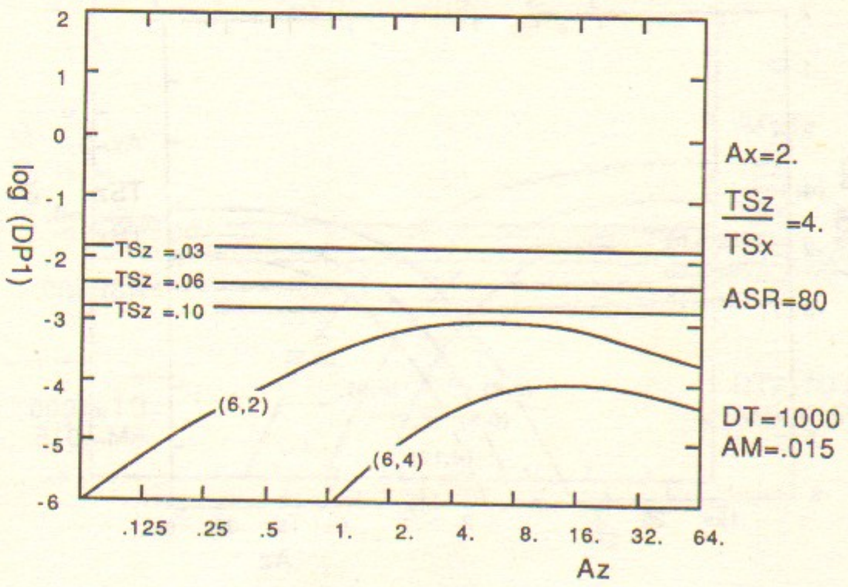

Figure 5b.4 Thresholds at Ax=2

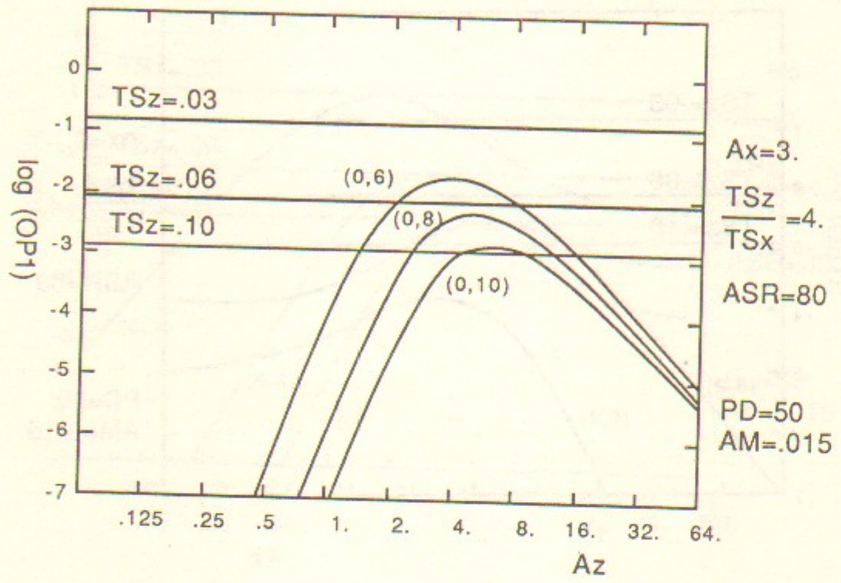

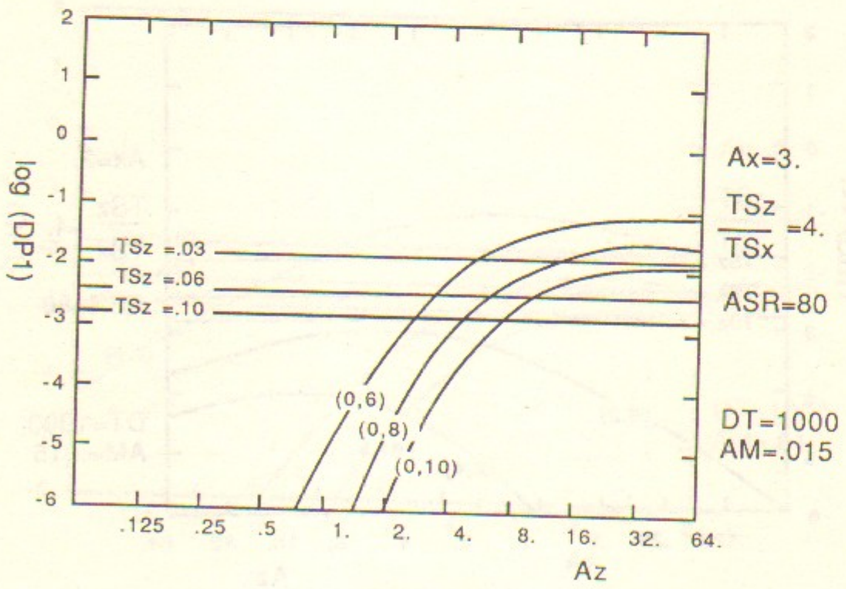

Figure 5c.1 Thresholds at Ax=3

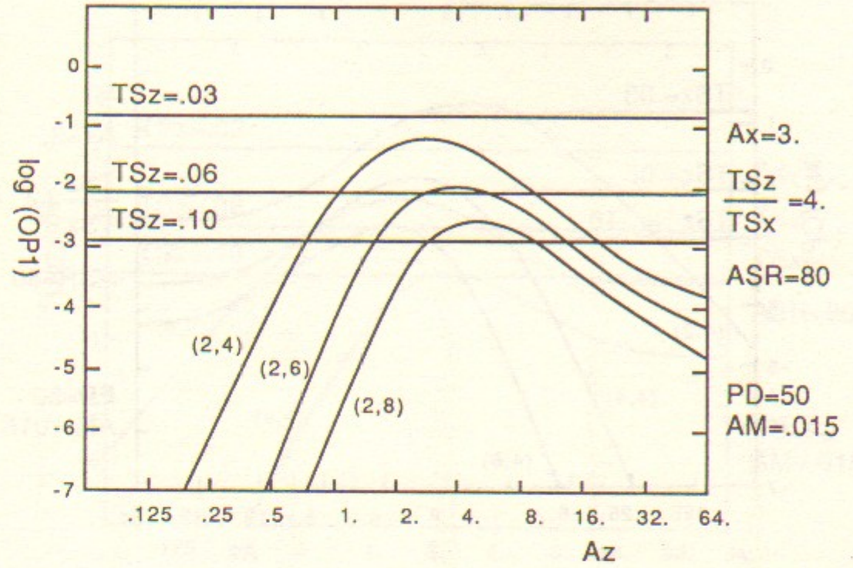

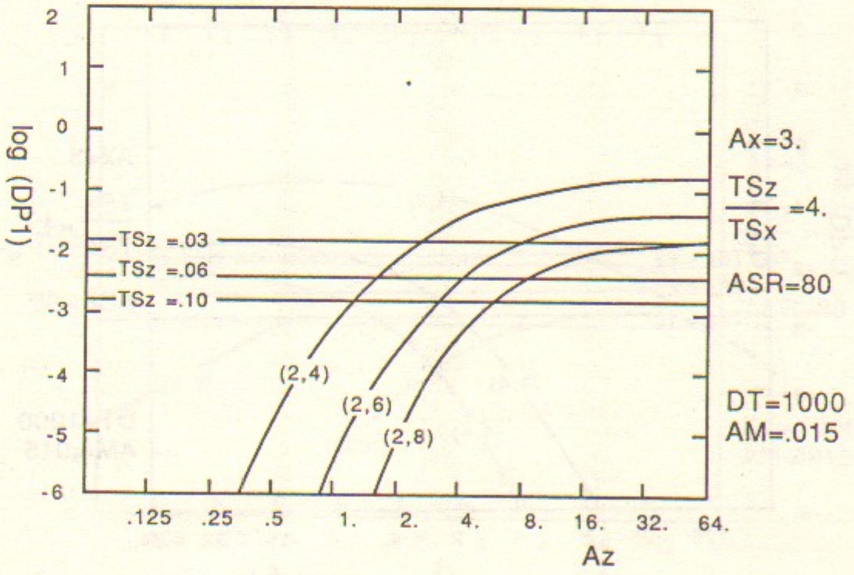

Figure 5c.2 Thresholds at Ax=3

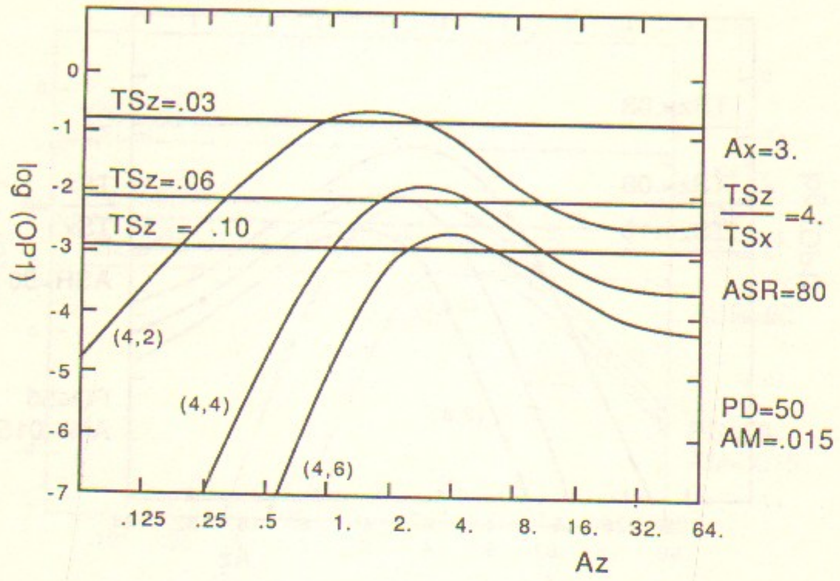

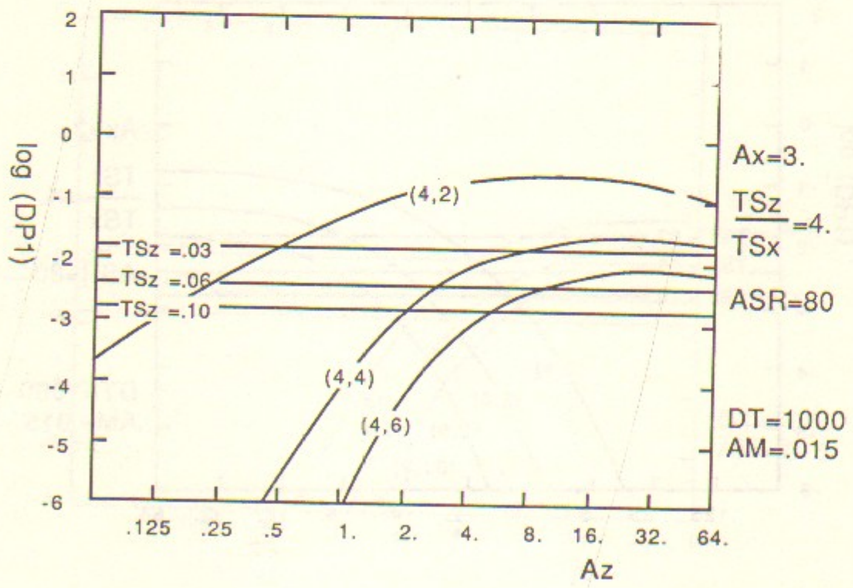

Figure 5c.3: Thresholds at Ax=3

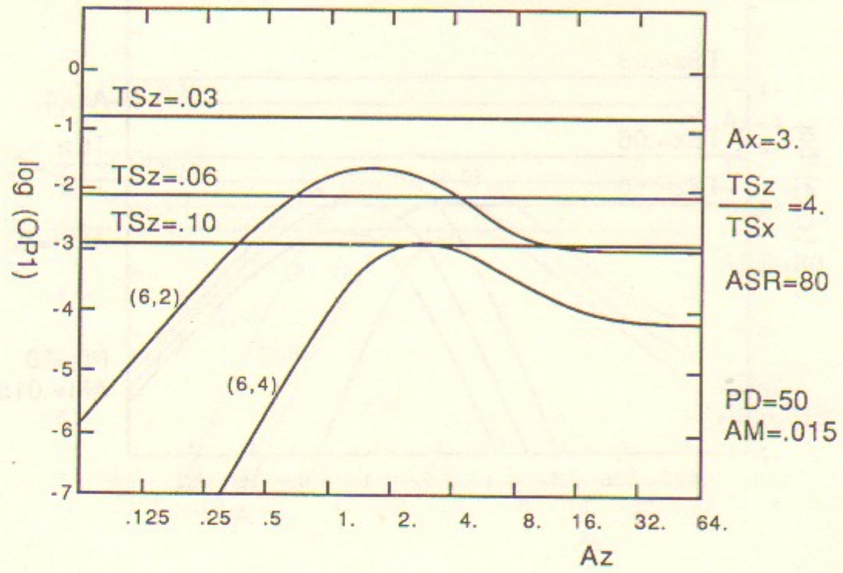

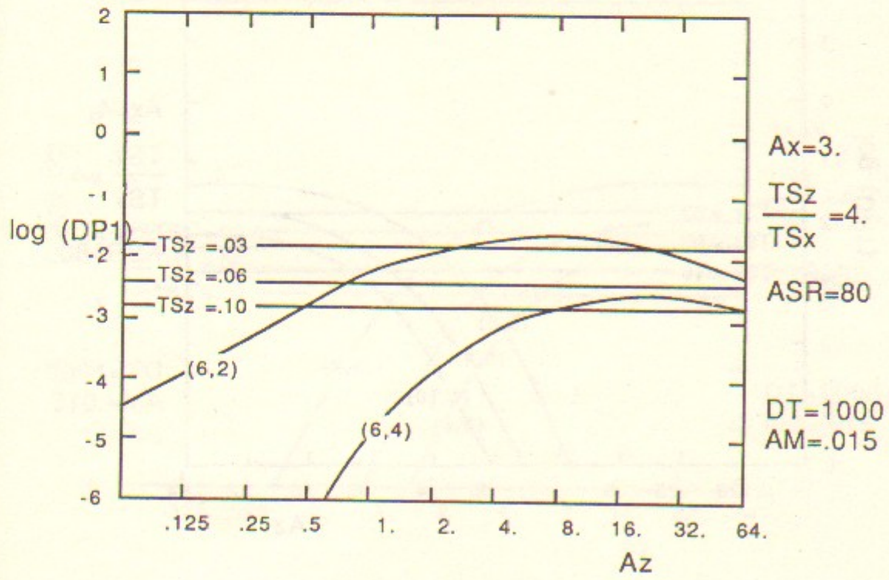

Figure 5c.4 Thresholds at Ax=3

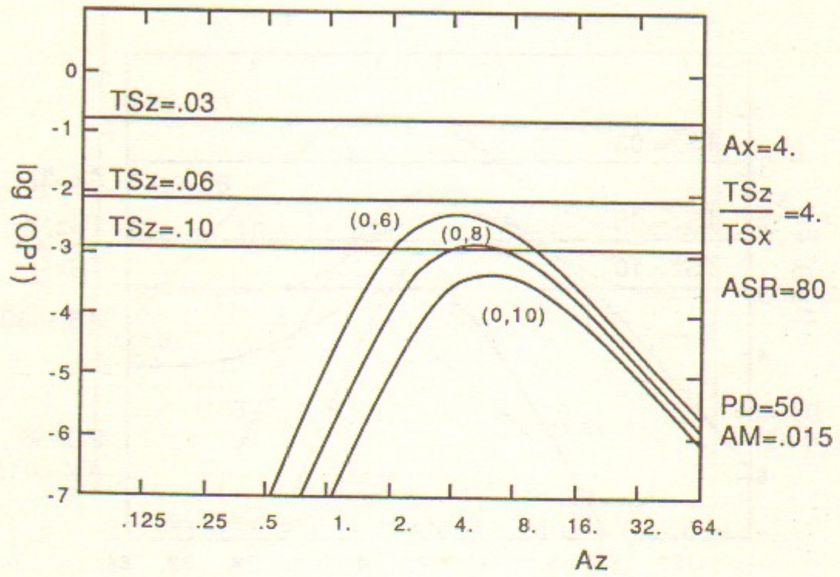

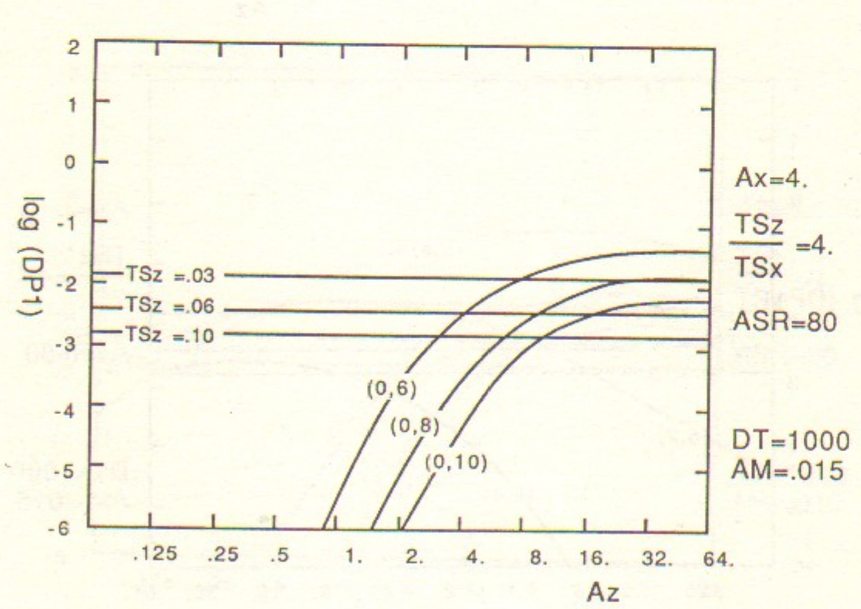

Figure 5d.1 Thresholds at Ax=4

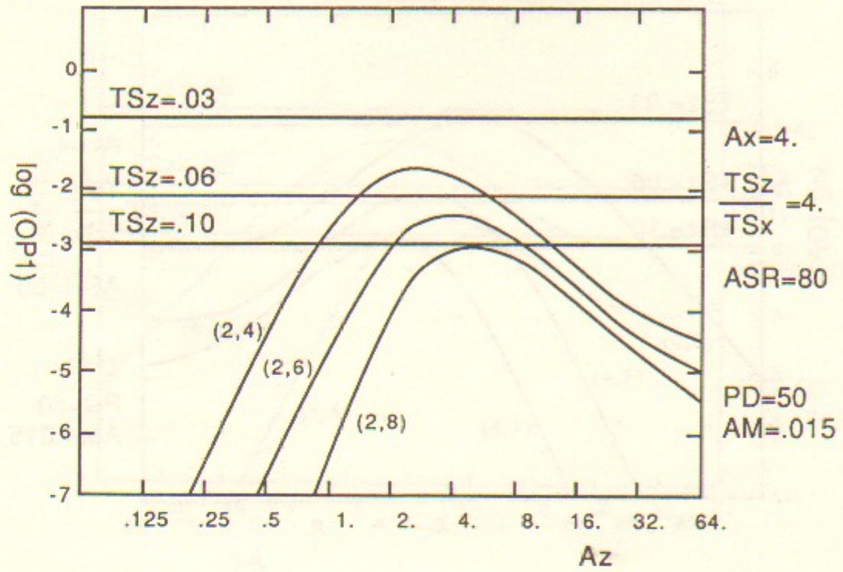

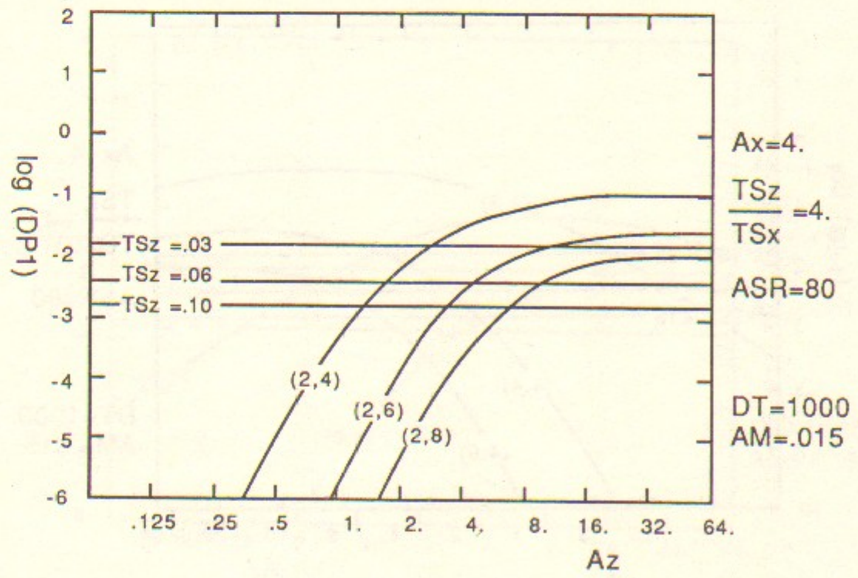

Figure 5d.2 Thresholds at Ax=4

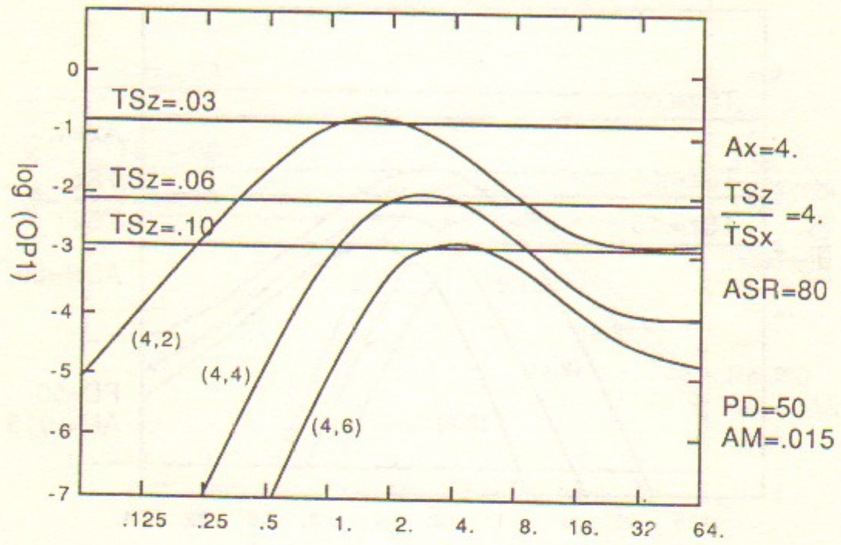

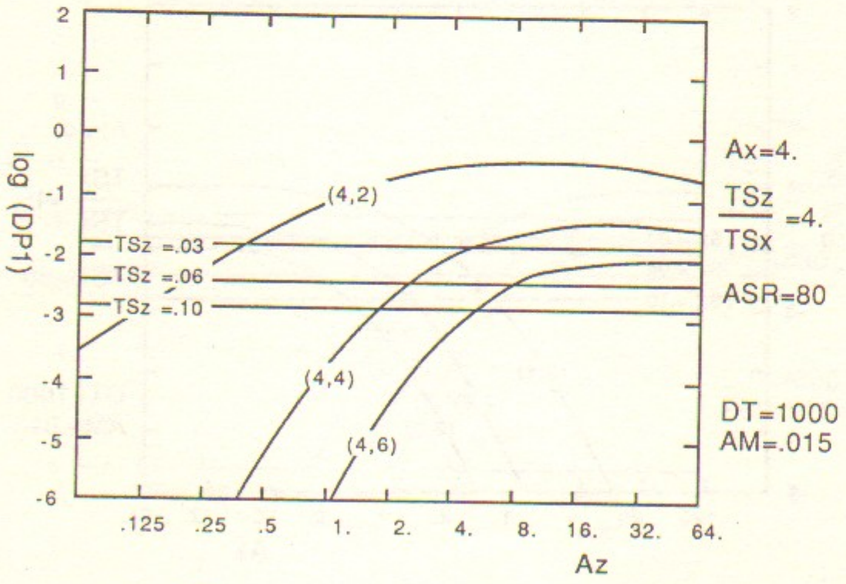

Figure 5d.3 Thresholds at Ax=4

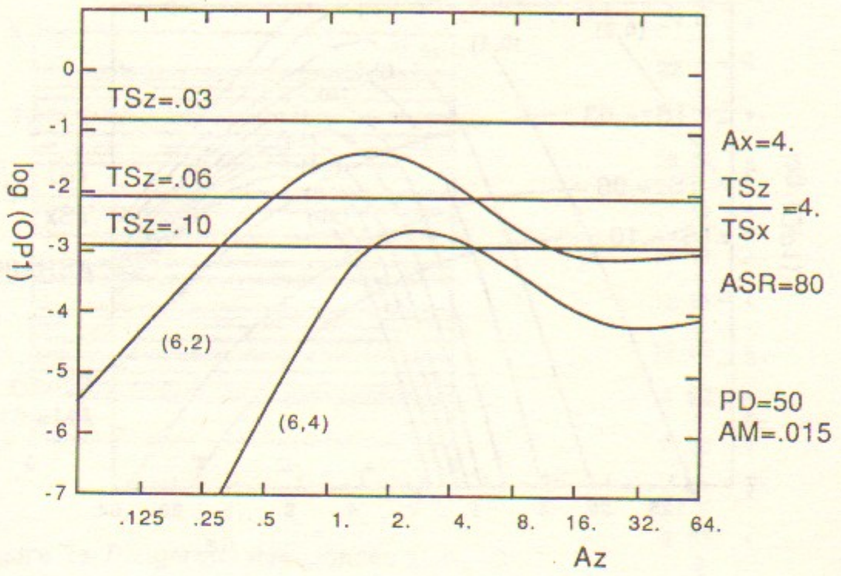

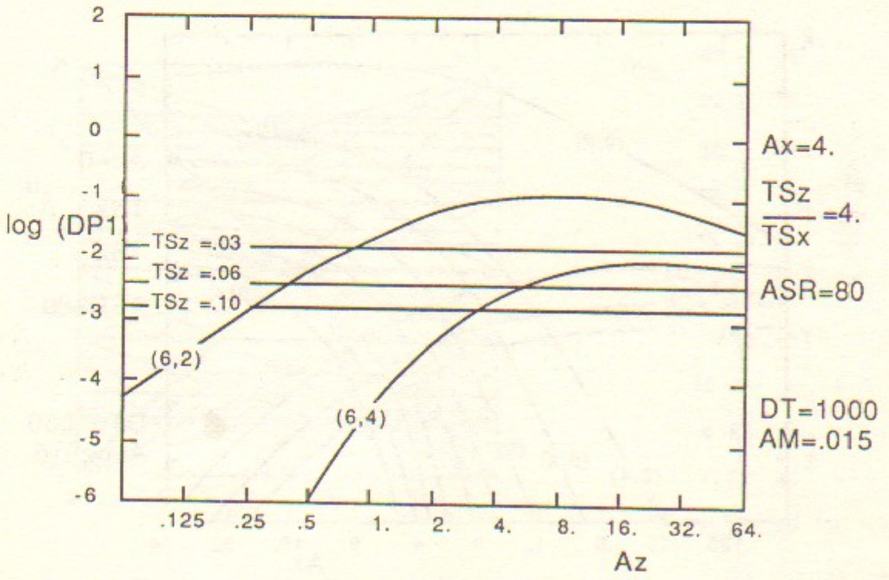

Figure 5d.4 Thresholds at Ax=4

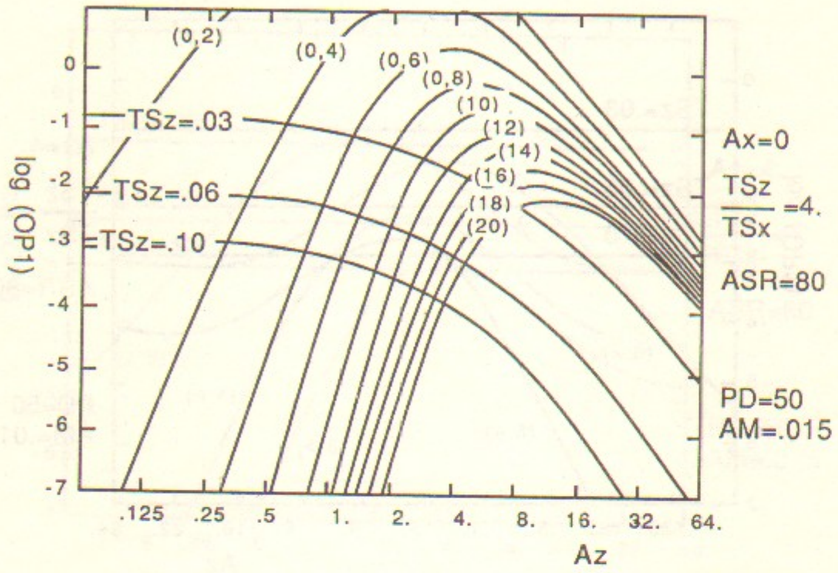

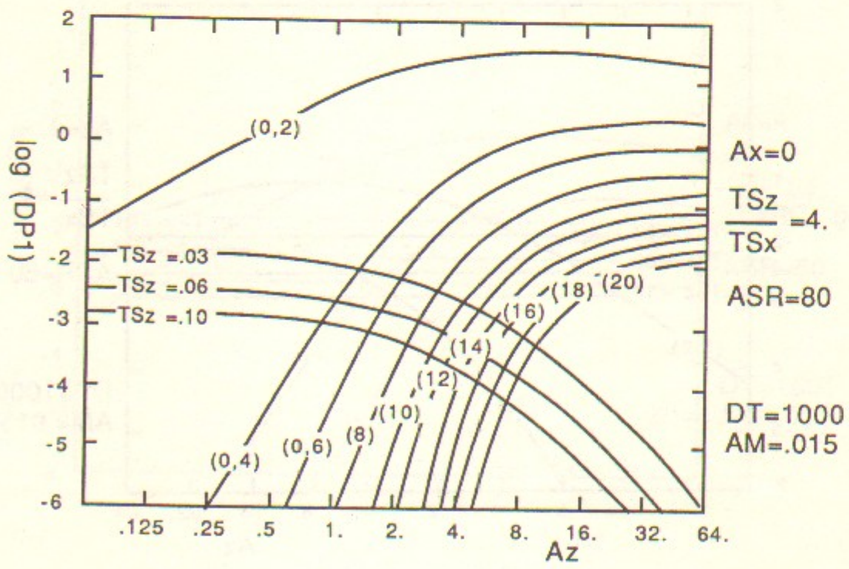

Figure 6. Thresholds at Ax=0 for tuneshift modulation

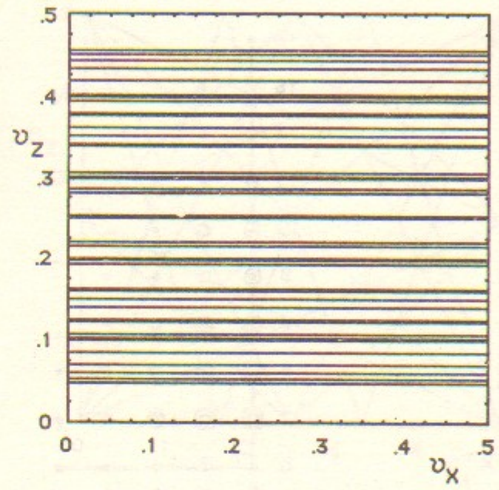

Figure 7a. Dangerous Resonances at A_x=0

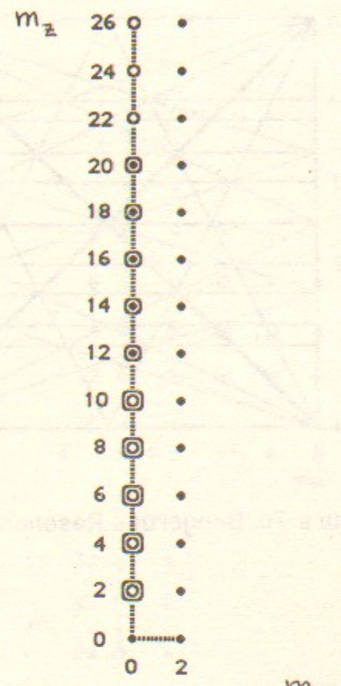

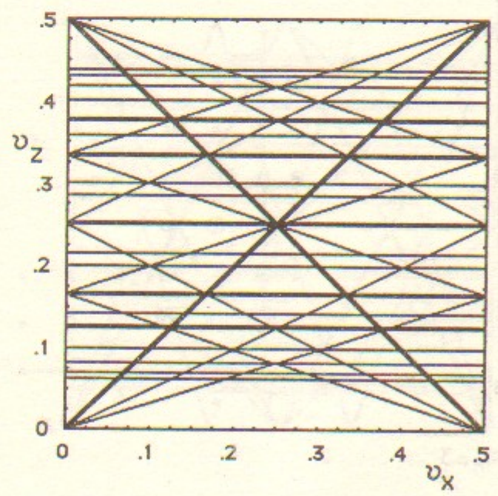

Figure 7b. Dangerous Resonances at A_x=1

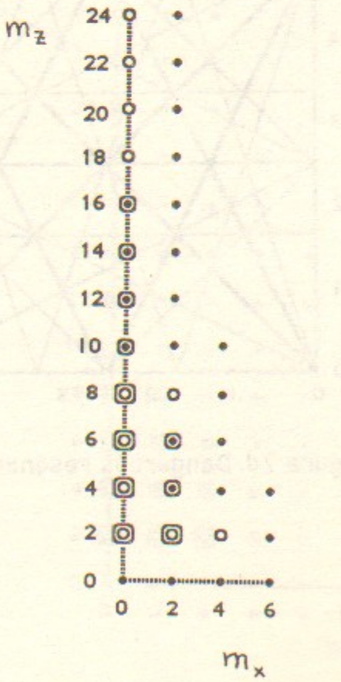

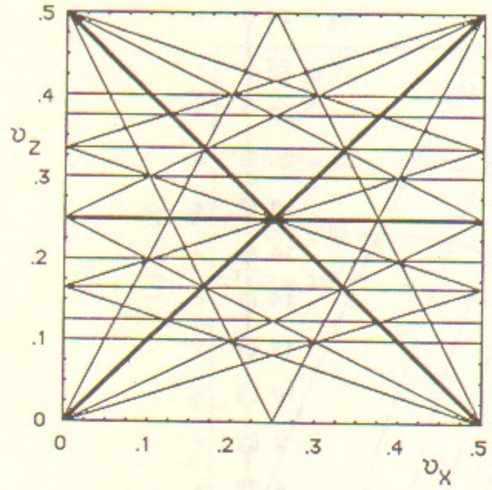

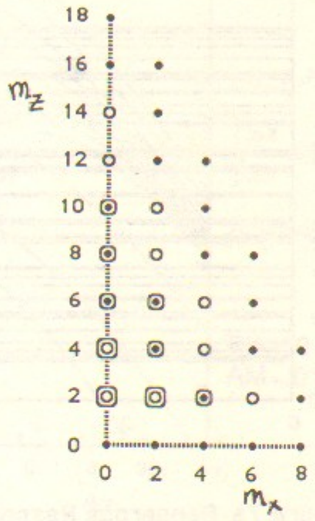

Figure 7c. Dangerous Resonances at A_X=2

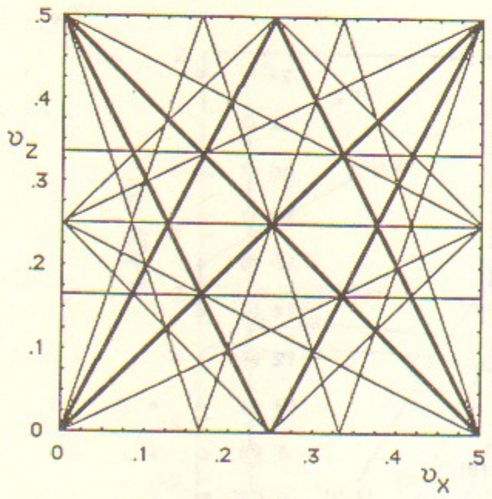

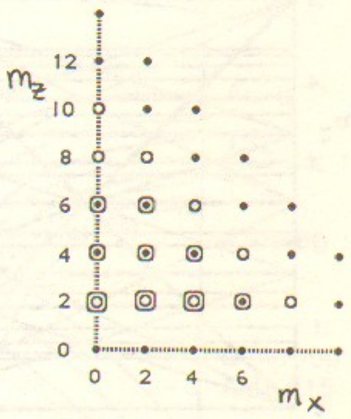

Figure 7d Dangerous resonances at A_X=3

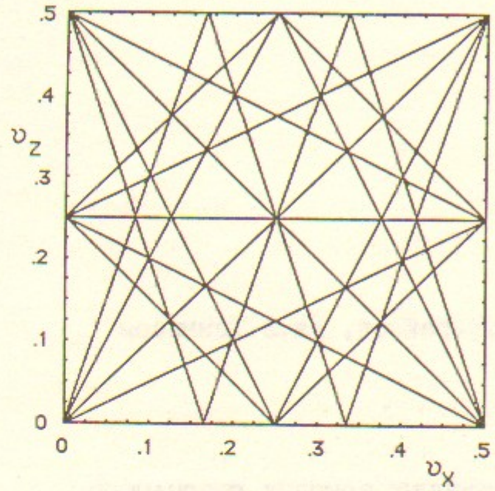

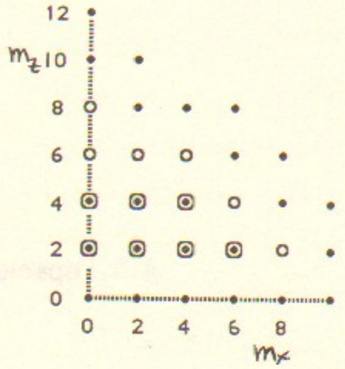

Figure 7e. Dangerous resonances at A_X=4

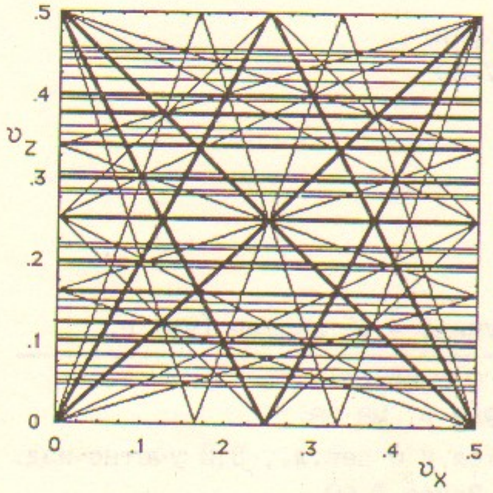

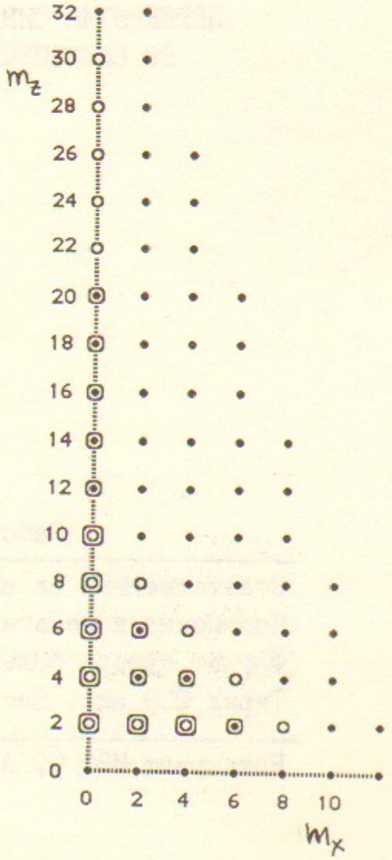

Figure 7f. All of the dangerous resonances

А.Л.Герасимов, Ф.М.Израйлев, Дж.Л.Теннисон

ПЕРЕКРЫТИЕ СИНХРОБЕТАТРОННЫХ БОКОВЫХ РЕЗОНАНСОВ ВО ВСТРЕЧНЫХ ЭЛЕКТРОН-ПОЗИТРОННЫХ ПУЧКАХ

Препринт
№ 87-69

Работа поступила - I5 апреля I987 г.

Ответственный за выпуск - С.Г.Попов
Подписано к печати 3.06.I987 г. МН 08215
Формат бумаги 60x90 I/I6 Усл.4,0 печ.л., 3,0 учетно-изд.
Тираж 230 экз. Бесплатно. Заказ № 69.

Ротапринт ИЯФ СО АН СССР, г.Новосибирск, 90